Dynamics of Water in Biological Recognition

Samir Kumar Pal and Ahmed H. Zewail*

Laboratory for Molecular Sciences, Arthur Amos Noyes Laboratory of Chemical Physics, California Institute of Technology, Pasadena, California 91125

Received August 12, 2003

Contents

1. Introduction 2099
2. Dynamics of Hydration: Theoretical 2103
   2.1. Bulk Solvation 2103
   2.2. Surface Hydration 2104
3. Bulk Hydration: Experimental 2106
   3.1. Methodology 2106
   3.2. Hydration Probes: Bulk Water 2107
      3.2.1. Tryptophan—Deciphering an Old Mystery 2107
      3.2.2. 2-(*p*-Toluidino)naphthalene-6-sulfonate in Bulk Water 2110
      3.2.3. 1-Anilinonaphthalene-8-sulfonate in Bulk Water 2110
      3.2.4. 2-Aminopurine in Water 2111
      3.2.5. Drug Hoechst 33258 in Bulk Water 2111
4. Proteins: Hydration and Function 2112
   4.1. The Enzyme Subtilisin *Carlsberg* 2112
   4.2. The Protein Monellin 2114
   4.3. The Enzyme α-Chymotrypsin 2115
5. DNA: Hydration and Function 2117
6. Conclusion 2120
7. Acknowledgment 2121
8. References 2121

1. Introduction

Almost all biological macromolecules—proteins (enzymes) and DNA—are inactive in the absence of water. Hydration of a protein/enzyme is particularly important for the stability of the structure and for the function, especially the recognition at a specific site. This role of hydration in enzyme catalysis is well known and has recently been reviewed in a number of publications.[1−3] In one of these studies it was shown that the dehydration of a protein, which makes it more rigid and increases its denaturation temperature, is correlated with the loss of its physiological function.[1]

The protein surface is complex, as many components are involved in describing hydration at the interface. Moreover, hydration by water has different spatial and temporal characteristics, defined by the landscape (surface topology, hydrophobic sites, etc.) of the macromolecule and by the kinetics (hydrogen bonding, transition state, etc.) of processes. Progress has been made and numerous experimental and theoretical studies[4−6] have been published. To elucidate the dynamical nature of interfacial water, however, the time scale must span the range from bulk-type behavior (femtosecond) and up to buried-water behavior (nanosecond or longer). An understanding of the dynamics of water molecules at the *surface* of proteins and DNA, with spatial (molecular) and temporal (femtosecond) resolution, was the goal of a series of publications from this laboratory.[7−11]

In one of the early investigations aimed at understanding the nature of proteins, Bernal and Crowfoot inferred from X-ray photographs of crystalline pepsin that protein molecules are relatively dense globular bodies with relatively large spaces that contain water.[12] Evidence of the omnipresence of water molecules in protein crystals came from the observation that the density of the crystalline form of proteins was less than that of the anhydrous form.[13] By using the flotation[14] of crystals in media of different densities, Adair and Adair[13] measured the density for a number of crystalline proteins including hemoglobin; for hemoglobin the density was found to be ∼1.23, definitely below the apparent density of the anhydrous protein in an aqueous solution, which was determined (∼1.3) by Svedberg.[15] This amounts[16] to hydration, in grams of water per gram of anhydrous protein, of ∼0.3 for hemoglobin.[13] The finding indicates that a significant amount of water remains attached to the protein; it defined water bound to proteins in solution as that which becomes unavailable as solvent to diffusible electrolytes.[13,17]

In his investigation of the molecular structure of hemoglobin, particularly the contacts at the interface between the subunits α_1 and β_1, Perutz[17] found that a significant number of water molecules play a role in bridging the globin subunits—from electron density maps, about 90 water molecules remain attached with each tetramer. However, this number is less than one-tenth that determined by Adair and Adair,[13] implying that a significant fraction of water molecules are attached too loosely to stay in one place during the long time it takes to collect X-ray diffraction data, presumably mostly due to surface water.[17,18] The role of "surface water" in protein stability and structure has been addressed theoretically in relation to the hydrophobic effect, with the emergence of the "iceberg model" [19] (see Figure 1).

* To whom correspondence should be addressed. E-mail: zewail@caltech.edu. Fax: (626) 792-8456.

10.1021/cr020689l CCC: $48.50
Published on Web 03/27/2004

Samir K. Pal was born (1970) in Sonamukhi near Kolkata, India. After receiving his B.Sc. (1991, University of Burdwan, India) and M.Sc. (1994, Jadavpur University, India) degrees in physics, he completed his Ph.D. work (2000) with Professor Kankan Bhattacharyya at the Indian Association for the Cultivation of Science (IACS). For the Ph.D. degree he mainly worked on picosecond dynamics (solvation, electron and proton transfer) of biomimetics (micelle, reverse micelle, hydro-gel, and vesicles). In March 2000, he joined the research group of Professor Ahmed H. Zewail at the California Institute of Technology. The focus of his study at Caltech is the fundamental ultrafast (femtosecond) processes (hydration, electron and energy transfer) in biological macromolecules, proteins, and DNA.

Ahmed H. Zewail received his B.S. and M.S. degrees from Alexandria University, and his Ph.D. from the University of Pennsylvania. After completion of his Ph.D., he went to the University of California, Berkeley, as an IBM research fellow. In 1976, he was appointed to the faculty at Caltech. Currently he is the Linus Pauling Chair Professor of Chemistry and Professor of Physics at the California Institute of Technology, and Director of the NSF Laboratory for Molecular Sciences (LMS). In the field of femtochemistry, developed at Caltech, elementary processes of chemical, physical, and biological changes are investigated with atomic-scale time resolution. His current research interests center on the development of ultrafast lasers and electrons for the studies of dynamics of complex structures and their functions. In 1999, he received the Nobel Prize in Chemistry for his scientific contribution to the field, and postage stamps have been issued for his contributions to science and humanity.

At the molecular level the questions of interest are many, and the following are pertinent to our interest here: (1) How rigid is the structure of water—the time scales? (2) How homogeneous is the distribution? (3) What is the degree of order, and how does ordered water influence the function? In general, these questions regarding structures and dynamics are also relevant to interfacial properties such as solvation,[20−22] molecular orientations at interfaces,[23] hydrophobic bonding,[24−27] and self-assembly.[28]

One of the early indications that the dynamics in the hydration layer of a protein is different from that of bulk water came from dielectric measurements.[4] Three distinct regions in the frequency-dependent dielectric function were found, in contrast to one region for bulk water, suggesting different types of water dielectric properties (see Figure 2). From these measurements it was found that the dielectric relaxation times (8.3 ps, 40 ps, 10 ns, 80 ns) of a protein in solution (myoglobin in this case) contrast that of bulk water (8.2 ps) at 298 K. The longer relaxation times, together with the Stokes expression of friction (from hydrodynamics), suggest a larger radius for the protein as a result of hydration. As discussed below, the existence of water hydration is now established by X-ray and neutron diffraction, and the time scales involved have been obtained on the subnanosecond scale using NMR and on the femtosecond−picosecond scale using ultrafast spectroscopy. On the theoretical side, molecular dynamics (MD) simulations have elucidated the range of binding energies and time scales.

Stimulated by neutron diffraction experiments,[29] MD simulations[30] indicate that typically about 80% of the hydration sites of carboxymyoglobin are occupied by water molecules, for a snapshot, and that only four water molecules remain bound during the entire length of the simulation (80 ps); see Figure 3. The residence time of water molecules in the hydration layer of this protein was found to have a distribution between somewhat less than 30 ps and about 80 ps, which was the longest run time of the simulation. A strong peak in the radial distribution function for hydrogen bonding (energy from 0.5 to 9 kcal/mol) to the surface was obtained, suggesting a "solvation shell" at an average distance of separation. The study of the trajectory of individual water molecules clearly shows two different behaviors—one for the bound and the other for the free water. Rapid exchange between the two states was also evident in the MD results,[30] suggesting the *existence of a dynamic equilibrium between the two states*. This equilibrium of two states was modeled kinetically to yield a residence time of this layer, termed by the authors as biological water.[31]

In another MD study of the dynamics of the protein plastocyanin,[32] a survival correlation time for the hydration layers was defined. This correlation function was allowed to decay only when water molecules leave or enter the layer; the function was found to decay slowly for the molecules that are close to the surface of the protein. As importantly, it was also observed that the *rotational relaxation* of the water molecules on average significantly slows down in the close proximity of the protein surface.

NMR studies of hydration belong to two classes of experiments;[33] those involve the nuclear Overhauser effect (NOE) between water, or counterion protons, and the specific proton of the macromolecule, and the nuclear magnetic relaxation dispersion (NMRD) of water, or counterions, of protein/DNA. The hydration studied by NOE techniques relies on relaxation-induced magnetization transfer between the dipolar coupled macromolecule and water protons.[34,35] This intermolecular magnetization transfer is formally described by a cross-relaxation rate (σ_{NOE}), which

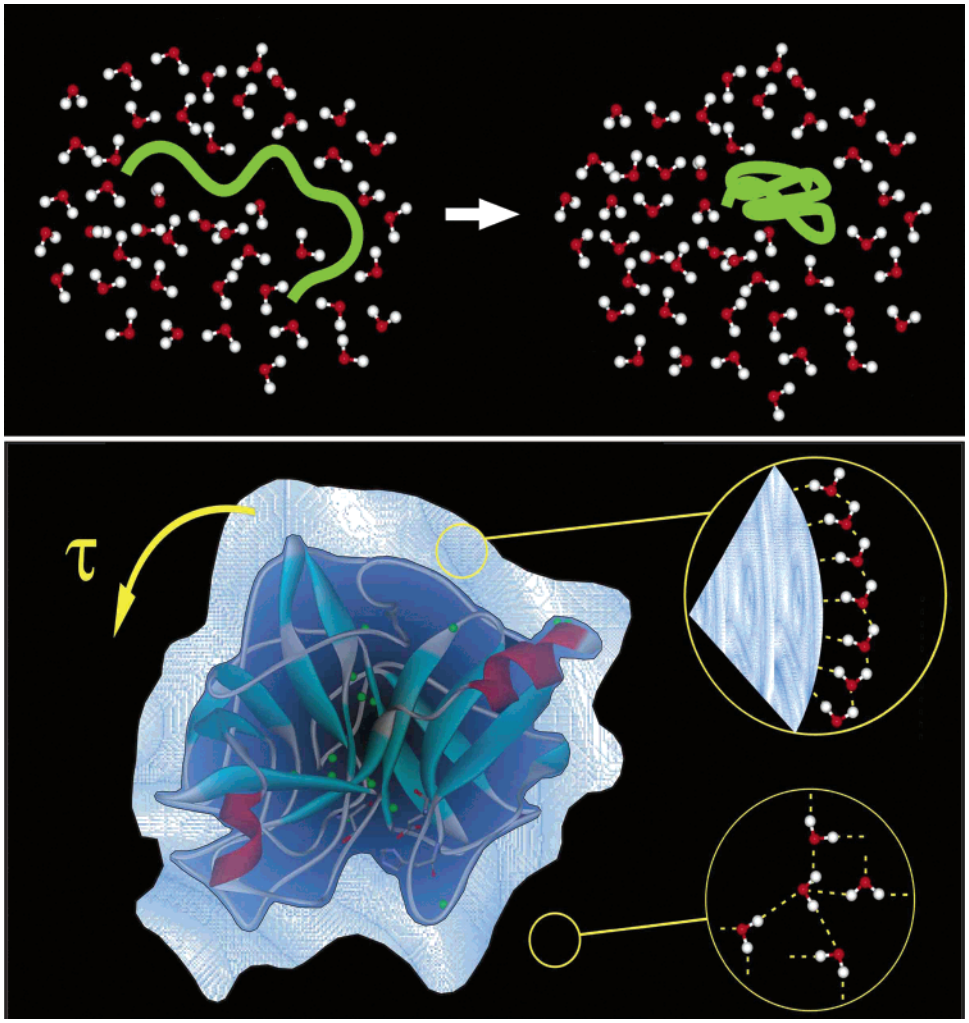

Figure 1. (Upper) Schematic for the role of water (hydrophobic effect) in changing the conformational state of a macromolecule. (Lower) Schematic representation of the iceberg model of a protein molecule, with a layer of strongly associated water (upper inset), suspended in aqueous solution. The hydration layer moves with the protein molecule (orientational relaxations, τ), and beyond this layer the water molecules adapt to the normal tetrahedral geometry (lower inset) and the orientational relaxation behavior of bulk water.

depends strongly on the intermolecular separation (r); in the rigid binding limit, $\sigma_{NOE} \approx 1/r^6$. Thus, all water protons within about 4 Å of a given macromolecular proton contribute significantly to the cross-peak.[33] This ability to spatially localize hydration sites is a major strength of the NOE method. The intrinsic limitation of the temporal resolution of NOE techniques makes accessible time resolution in the subnanosecond scale, reporting 500 ps to 300 ps.[34,35]

In a typical NMRD study of macromolecular hydration,[33,36] the longitudinal magnetic relaxation rate of the deuteron or oxygen-17 nucleus in the water molecule is measured as a function of resonance frequency (i.e., applied static magnetic field). Water molecules of the protein or DNA exchange rapidly (on the relaxation time scale) with the bulk water, and every water molecule in solution contributes. From the frequency dependence it is possible to reach a shorter time resolution, reported to be in the range of 10−50 ps.[36] As pointed out by Halle,[36] the inherent lack of spatial resolution and the complications of hydrogen exchange make the molecular interpretation a subject of discussion.

The above issues regarding the hydration of proteins are of similar importance to DNA hydration. Hydration of DNA plays an important role in its structure, conformation, and function. Of significance to the function is the selective recognition by DNA of small molecules.[37] Studies of X-ray crystallography, thermodynamics, NMR, dielectric relaxation, and molecular dynamics simulation have shown that a significant amount of water molecules are bound to DNA (for reviews, see refs 33, 38−42). For example, measurements of dielectric relaxation due to water molecules bound to DNA in mixed water−ethanol solutions have found that 18−19 water molecules per nucleotide are present in B-DNA, but only 13−14 water molecules are bound in A-DNA.[40] The same study also suggested that a structural transition of poly(dG-dC)·poly(dG-dC) DNA from its B to Z form takes place upon the removal of the bound water molecules, preferentially from the phosphate groups.

The molecular picture of hydration in the minor groove of B-DNA is unique. An X-ray crystallographic investigation[43] followed by a solution NMR study[44] on a model dodecamer B-DNA duplex showed that

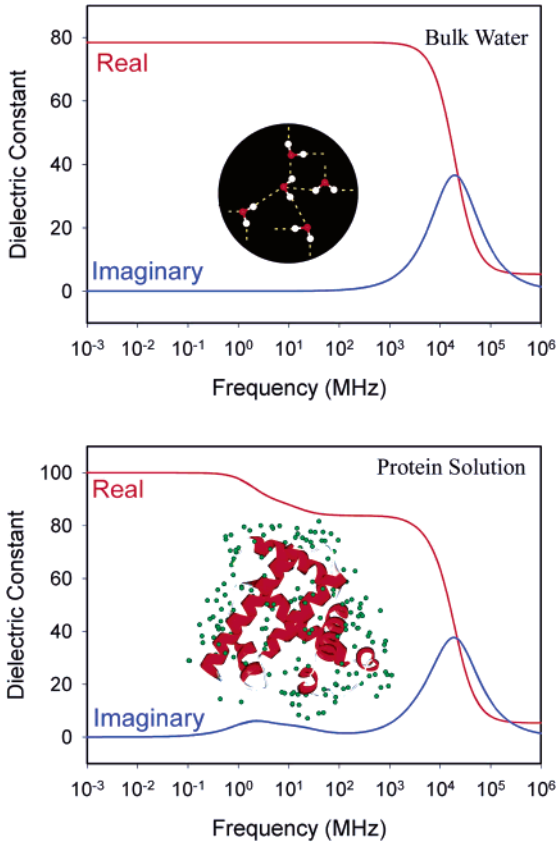

Figure 2. Frequency dependence of the real and imaginary parts of the dielectric constant as manifested in dielectric dispersion of bulk water (upper panel) and aqueous protein (myoglobin) solution (lower panel) at 298 K. Data were generated numerically by using the parameters obtained from dielectric measurements of bulk water and protein solution at 298 K. The dispersion formula and the parameters used are described in Chapter 4 of ref 4. Note that a conversion to angular frequencies (and fit of the dispersion) is needed in order to obtain relaxation times.

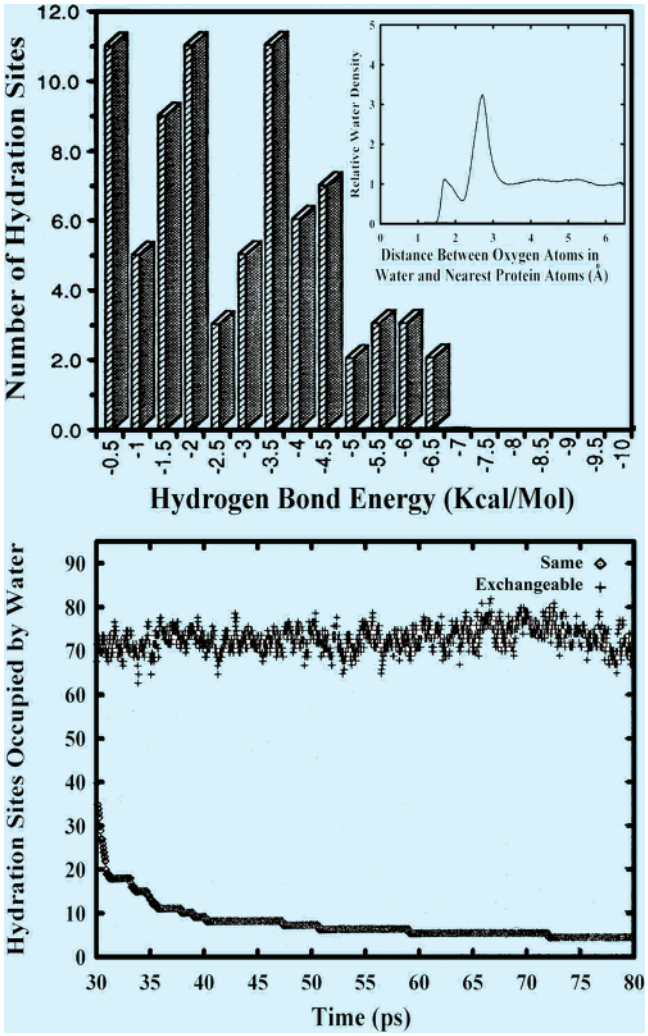

Figure 3. (Upper) Distribution of hydrogen bond energies for the 89 hydration waters determined from neutron diffraction of the protein carboxymyoglobin. Inset: Water−protein radial distributions. (Lower) The number of hydration sites observed in the MD simulation based on hydration waters shown by the neutron diffraction experiment. The bottom curve shows the number of hydration sites occupied by the same water at each time step of the simulation. The time interval is 0.04 ps. The top curve shows the number of hydration sites occupied by water at a given time step. Reprinted with permission from ref 30. Copyright 1995 Wiley-Liss, Inc., a subsidiary of John Wiley & Sons, Inc.

the minor groove is hydrated in an extensive and regular manner, with a zigzag "spine" of first and second shell hydration along the floor of the groove. In contrast, hydration within the major groove is principally confined to a monolayer of water molecules. The conformational energy calculation suggested that the presence of the spine of hydration is the prime reason for the further narrowing of the minor groove.[45] The nanosecond dynamics of hydration of DNA have been reported, primarily for the spine water in the minor groove.[33]

In this article, we will review the work at Caltech on hydration dynamics on the femtosecond time scale for the protein monellin and enzymes subtilisin *Carlsberg* and α-chymotrypsin, and for two types of DNA (dodecamer duplex and calf thymus). The spatial resolution in these experiments is determined by the selection of a specific molecular site (tryptophan and ANS in the case of proteins and the drug Hoechst 33258 in the case of DNA complexes). The site structure is known from X-ray crystallography, and it is the one probed following femtosecond excitation, which defines the zero of time for water translational and rotational motions in the layer. We will discuss the dominance of hydration by water over other polar side chains and give an estimate of the layer thickness by varying the distance (∼1 nm) of the probe from the surface. From studies of the pH dependence of the enzyme α-chymotrypsin, we propose a role of hydration in its function. For DNA, we examine the interfacial water involved in the drug recognition in the minor groove, and whose complex structure is determined by X-ray crystallography. We also summarize the findings of a simple theoretical model developed to provide a relationship between the hydration correlation time(s) and the residence time(s) of water molecules. We will not discuss related works from this laboratory, which focused on other aspects of dynamics such as energy transfer, electron and proton transfers, and ligand recognition (see conclusion).

2. Dynamics of Hydration: Theoretical

2.1. Bulk Solvation

To understand the meaning and scope of solvation dynamics, let us first visualize the physical picture of the dynamical process involved for a solute molecule in a polar solvent.[46−48] A change in the solute is made at time $t = 0$, by femtosecond excitation, which leads to the creation of a dipole. This dipole gives rise to an instantaneous electric field on the solvent molecules. Because of the interaction of the solvent permanent dipoles with the electric field, the free energy minimum of the solvent shifts to a nonzero value of the polarization. The solvent motion is critical. Since the solute is excited instantaneously (a Franck−Condon transition as far the nuclear degrees of freedom are concerned), the solvent molecules at $t = 0$ find themselves in a relatively high-energy configuration. Subsequently, the solvent molecules begin to move and rearrange themselves to reach their new equilibrium positions (Figure 4, upper). The nuclear motion involved can be broadly classified into rotational and translational motions.

When the solvent is bulk water, rotational motion would also include hindered rotation (libration), while translation would include the intermolecular vibration due to the extensive hydrogen bonding. The two specific motions, libration and intermolecular vibration, are relatively high in frequency and are expected to play a dominant role in the initial part of solvation.[49] In Figure 4 (lower) we show results[8] of a theoretical study of the behavior of the correlation function which we shall discuss below. For clarity, we approximate the motions responsible for decay in different regions.

The time dependence of the solvation energy is determined by the time dependence of polarization, which is in turn determined by the time dependence of the density: $\mathbf{P}(\mathbf{r},t) = \int d\mathbf{\Omega}\ \boldsymbol{\mu}(\mathbf{\Omega})\ \rho(\mathbf{r},\mathbf{\Omega},t)$, where $\boldsymbol{\mu}(\mathbf{\Omega})$ is the dipole moment vector of a molecule at position $\mathbf{r}$, and $\rho(\mathbf{r},\mathbf{\Omega},t)$ is the position, orientation, and time-dependent density. If the perturbation due to the probe on dynamics of bulk water is negligible, then the time dependence of polarization is dictated by the natural dynamics of the liquid. The theoretical analysis of the time-dependent density is usually carried out by using a molecular hydrodynamic approach that is based on the basic conservation (density, momentum, and energy) laws and includes the effects of intermolecular (both spatial and orientational) correlations. The latter provides the free energy surface on which solvation proceeds. The equation of motion of the density involves both orientational and translational motions of the solvent molecules.[48,50−52]

Within linear response theory, the solvation time correlation function is directly related to the solvation energy:

$$C(t) = \frac{\langle \delta E(0)\delta E(t)\rangle}{\langle \delta E^2\rangle} = \frac{\langle E(t)\rangle - \langle E(\infty)\rangle}{\langle E(0)\rangle - \langle E(\infty)\rangle} \qquad (1)$$

where δE is the fluctuation of solvation energy from the average, equilibrium value. Note that the equality in eq 1 indicates a direct relation between the average of the fluctuations over the equilibrium distribution (left) and the nonequilibrium function (right), which relates to observables; $\langle E(\infty)\rangle$ is the result of the equilibrium term in the numerator and for normalization in the denominator.[8]

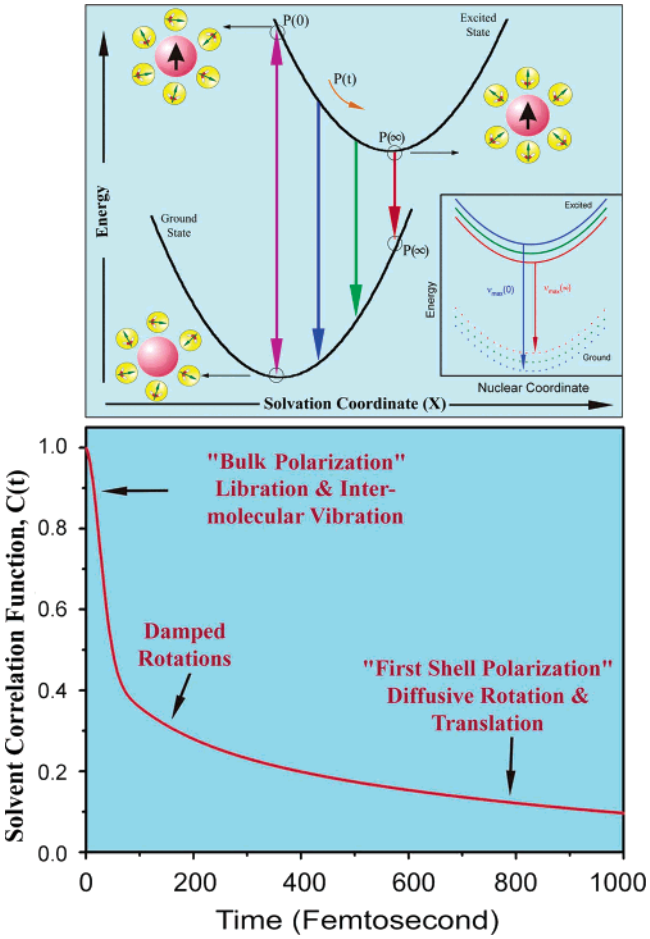

Figure 4. (Upper) Schematic illustration of the potential energy surfaces involved in solvation dynamics, showing the water orientational motions along the solvation coordinate together with instantaneous polarization P. Inset: The change in the potential energy along the intramolecular nuclear coordinate. As solvation proceeds, the energy of the solute decreases, giving rise to a red shift in the fluorescence spectrum. Note the instantaneous P, e.g., $P(\infty)$, on the two connected potentials. (Lower) A typical solvation time correlation function for water is shown. The time correlation function exhibits three distinct regions: the initial ultrafast decay, an intermediate decay of about 200 fs, and the last slow decay with a time constant of 1 ps. The physical origin of each region is indicated on the plot itself; see text.

The ultrafast component in the solvation time correlation function (see Figure 4) originates from the initial relaxation in the steep collective solvation potential. The collective potential is steep because it involves the total polarization of the system.[46,48] This initial relaxation couples mainly to the hindered rotation (that is, libration) and the hindered translation (that is, the intermolecular vibration), which are the available high-frequency modes of the solvent; neither long-amplitude rotation nor molecular trans-

lation is significant here. The last part in the decay of the solvation correlation function involves larger amplitude rotational and translational motions of the nearest-neighbor molecules in the first solvation shell. In the intermediate time, there are contributions from the moderately damped rotational motions of water molecules. In a sense, with the above description one recovers the famous Onsager's "inverse snowball" picture of solvation.[53] A simple but fairly accurate way to describe the slower part of the solvation dynamics (which involves rearrangement of the solvent molecules that are the nearest neighbors of the probe) is to use a wave-vector-dependent relaxation time, as is routinely used in the description of neutron scattering experiments, and this is discussed elsewhere.[8]

From the behavior of the correlation function of hydration and the numerical estimate,[8] the picture is clear. The slowest time constant is about 1 ps, which is determined by the individual rotational and translational motions of the molecules in the "first solvation shell" rather close to the probe. The femtosecond component is dominated by the high-frequency hindered rotational and translational (vibration)[49,54,55] polarization. A wave packet formulism can be developed to describe the transient behavior for the population during solvation.[8] The picture is rather simple using the potentials of solvation in Figure 4 (upper).

Conceptually, it is clear how the change in energy can map out the time scale of the motion of the solvent. By following the change of transients with wavelength of emission (excited-state energy), we can probe the relaxation process on the solvent coordinate of the free energy surface. The emission transients detected in the blue region (higher energy) of the emission spectrum will be characterized by decay components reflecting forces of motion. When detection is redder (lower energy), however, the decay part slows until eventually a rise is observed. The time scales of decay and rise in the blue and red regions, respectively, depend on the temporal behavior of relaxation on the solvation energy surface (Figure 4). Repeating these experiments for the entire range of energies available, we can obtain $C(t)$ and the hydration dynamics. The orientation of the probe and its rigidity can be studied using the change in emission anisotropy with time, as discussed below.

2.2. Surface Hydration

The solvation dynamics of an external probe located at the surface or in hydrophobic pockets/clefts of a protein (or DNA) is rather complex because it involves contributions from spatial and temporal inhomogeneities. Experiments have shown, using coumarin[56] or eosin[57] as an extrinsic dye probe, that a multiphasic behavior is present but still with short- and long-time components. In one such study, the observed relaxation (for coumarin) was attributed entirely to a hydrophobic pocket in the inside solvent-inaccessible region.[56] For the other probe (eosin),[57] the X-ray structure (see below) indicates that it is in a hydrophobic pocket. Even with a natural probe,[7] we must consider the different contributions to solvation, the protein molecule, the water in the hydration shell, and the bulk water, but we can eliminate the inhomogeneity in bindings and the local structural changes due to a foreign probe.

For DNA, studies of solvation dynamics have been reported for a chromogenic probe, inserted into DNA either by covalent adduction (coumarin dye)[58] or by hydrophobic intercalation (acridine dye).[59] The fluorescence results[58] give relaxation time constants of 300 ps (47%) and 13 ns (53%), both measured with 100 ps time resolution and attributed to the local reorganization (by DNA and/or water) in the modified DNA. The results from femtosecond-resolved transient absorption[59] suggest an ultrafast (within 200 fs) "repolarization" of the nuclear degrees of freedom of the DNA pocket. However, the lack of information on the structures of the two complexes keeps the extent of perturbation on DNA unknown. Moreover, neither study gave the hydration dynamics in the DNA grooves.

In the following we consider the different processes involved in protein hydration, with the following questions in mind: What is the microscopic origin of the long-time solvation dynamics? If the slow solvation arises from the hydration layer, then why does the 1 ps component persist? What is the residence time and its distribution, and why does it affect the friction by translational and rotational motions? And finally, what about solvation by protein residues?

As mentioned above, we consider two types of water, those bound to the surface and those that are free. The equilibrium between the two types is determined by the time scale,[8,30,31] as depicted in Figure 5. In the water layer around the protein surface, the interaction with water involves hydrogen bonding to the polar and charged groups of the surface. The strength of this bonding varies from group to group. When strongly bonded to the protein, the water molecules cannot contribute to solvation dynamics because they can neither rotate nor translate. But the hydrogen bonding is transient, and there is a dynamic equilibrium between the free and the bound water molecules. The potential of interaction can be represented by a double-well structure to symbolize the processes of bond breaking and bond forming.

In general, the bonded water molecules become free by translational and rotational motions. The experimental observations of a biphasic behavior of hydration (see the experimental section) indicated the presence of "bound" and "free" water in the surface layer, and this stimulated a theoretical treatment of the change of density with time. In the simplest model, the exchange was considered only in the layer.[8] Two coupled reaction−diffusion equations were solved. The two rate constants, k_{bf} and k_{fb}, were introduced to describe the transition from bound (to the surface) to free (from the surface) and the reverse, respectively:

$$\textbf{bound} \leftrightarrows \textbf{free} \quad \textbf{(rotating and translating)}$$

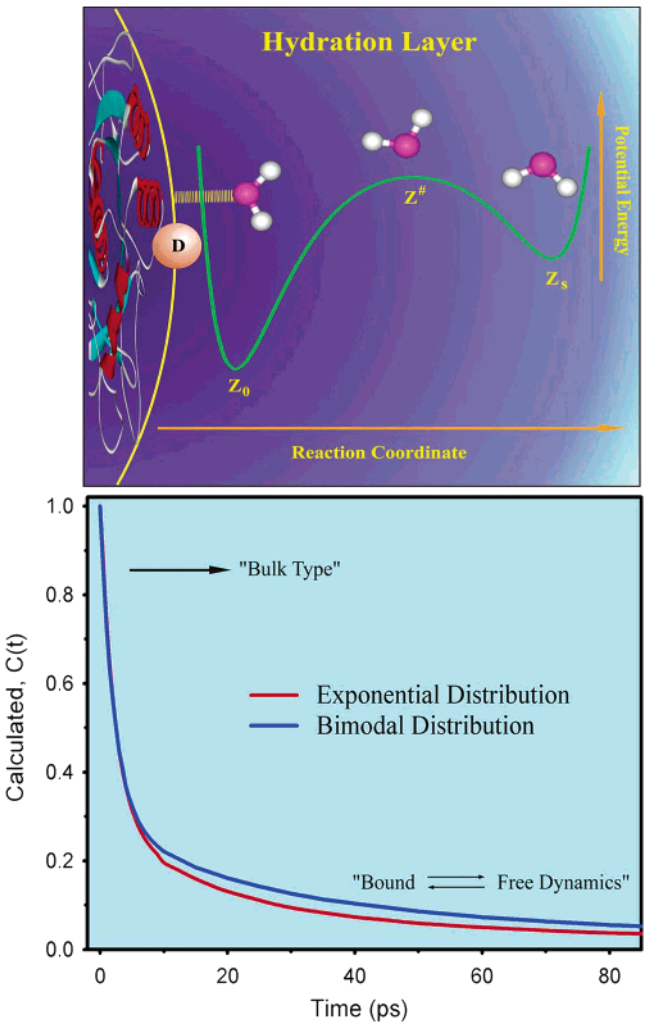

Figure 5. (Upper) Illustration of the dynamic equilibrium in the hydration layer of a protein. The potential for the exchange is shown. (Lower) The calculated hydration correlation functions for two distributions of water bonding in the layer; see text for the theoretical discussion.

Thus, two equations can express the change of density with time:

$$\frac{\partial}{\partial t}\rho_f(\mathbf{r},t) = D_T\nabla^2\rho_f(\mathbf{r},t) + D_R\nabla^2\rho_f(\mathbf{r},t) - k_{fb}\rho_f(\mathbf{r},t) + k_{bf}\rho_b(\mathbf{r},t) \quad (2)$$

$$\frac{\partial}{\partial t}\rho_b(\mathbf{r},t) = -k_{bf}\rho_b(\mathbf{r},t) + k_{fb}\rho_f(\mathbf{r},t) \quad (3)$$

where ρ_f and ρ_b are the densities of the free and the bound water molecules, respectively. The equations were solved for the polarization to find two wave-vector-dependent relaxation times ($\tau_\pm$); the solution in the limit of large activation barrier between the bound and free states is straightforward. This is because $(\tau_s^{bulk}(k))^{-1}$ is close to 10^{12} s^{-1} and the transition rates, k_{bf} and k_{fb}, are expected to be smaller. In this case,[8] the time constants are given by

$$\tau_{fast} \equiv |\tau_-| \approx \tau_s^{bulk} \quad (4a)$$

$$\tau_{slow} \equiv |\tau_+| \approx k_{bf}^{-1} \quad (4b)$$

In the same limit of large activation energy separating the bound state from the free one, the residence time of the bound water molecules is given essentially by k_{bf}^{-1}, which is in the range of tens of picoseconds.

The above model was further developed[60] to take into account the effect of the bulk water re-entry to the layer—which we termed a feedback mechanism—and the role of orientational order and surface inhomogeneity in the observed decay characteristics. With this in mind, the expressions for the change in density with time can be written as follows:

$$\frac{\partial}{\partial t}\rho_f(\mathbf{r},\mathbf{\Omega},t) = D_T\nabla^2\rho_f(\mathbf{r},\mathbf{\Omega},t) + D_R\nabla^2\rho_f(\mathbf{r},\mathbf{\Omega},t) - [(\rho_f(\mathbf{r},\mathbf{\Omega},t)\int d\mathbf{\Omega}_1\, k_{fb}(\mathbf{\Omega},\mathbf{\Omega}_1) - \int d\mathbf{\Omega}_1\, \rho_b(\mathbf{r},\mathbf{\Omega}_1,t)k_{bf}(\mathbf{\Omega}_1,\mathbf{\Omega})]h(z_l - z) \quad (5)$$

$$\frac{\partial}{\partial t}\rho_b(\mathbf{r},\mathbf{\Omega},t) = -\rho_b(\mathbf{r},\mathbf{\Omega},t)\int d\mathbf{\Omega}_1\, k_{bf}(\mathbf{\Omega}_1,\mathbf{\Omega}) + \int d\mathbf{\Omega}_1\, \rho_f(\mathbf{r},\mathbf{\Omega}_1,t)k_{fb}(\mathbf{\Omega},\mathbf{\Omega}_1) \quad \text{at} \quad 0 < z < z_l \quad (6)$$

where $k_{fb}(\mathbf{\Omega},\mathbf{\Omega}_1)$ is the transition rate from free water with orientation $\mathbf{\Omega}$ to bound water with orientation $\mathbf{\Omega}_1$. Similarly, $k_{bf}(\mathbf{\Omega}_1,\mathbf{\Omega})$ denotes a transition rate from bound water with orientation $\mathbf{\Omega}_1$ to free water with orientation $\mathbf{\Omega}$. Bound water exists only in the surface layer (width z_l), and this is taken into account by the presence of the Heaviside step function, $h(z_l - z)$, which is one for positive argument (layer) and zero for the negative value (bulk). The picture is elucidated in Figure 6 and can be written as

layer bound ⇆ layer free ⇔ bulk free

with the degree of orientation defined by Ω and the layer thickness by z_l. The solutions, which involve the use of spherical harmonics expansion (for orientational distributions) and Green's function in Laplace space, give[60] the biphasic behavior with the two rates defined as follows:

$$\tau_{fast} = \frac{1}{(2D_R + Dq^2)} \quad (7)$$

which is similar in form to that given previously (q is the wavenumber and D is the translational diffusion coefficient; see eq 4 of ref 8) and describes the ultrafast (~1 ps) decay at early times. In bulk, the orientational relaxation time (τ_{or}) is 2.6 ps[61] and $D_R = 1.9 \times 10^{11}$ s^{-1}, with D_R being equal to $(2\tau_{or})^{-1}$.

However, the slow relaxation time now takes the following form:

$$\tau_{slow} = \frac{1}{k_{bf}}\left[1 + (k_{fb}\tau_{fast})^{1/2}\frac{z_l}{\lambda}\right] \quad (8)$$

where $\lambda = (D/k_{fb})^{1/2}$. Clearly, as in the previous model,[8] τ_{slow} and k_{bf} are directly related. But the additional term indicates that there is a contribution from the bulk feedback process. When z_l and λ become on the order of the molecular dimension and $k_{fb}\tau_{fast} \approx 1$, the maximum value is $\tau_{slow} \approx 2(k_{bf}^{-1})$. The numerical results, the effect of the degree of orienta-

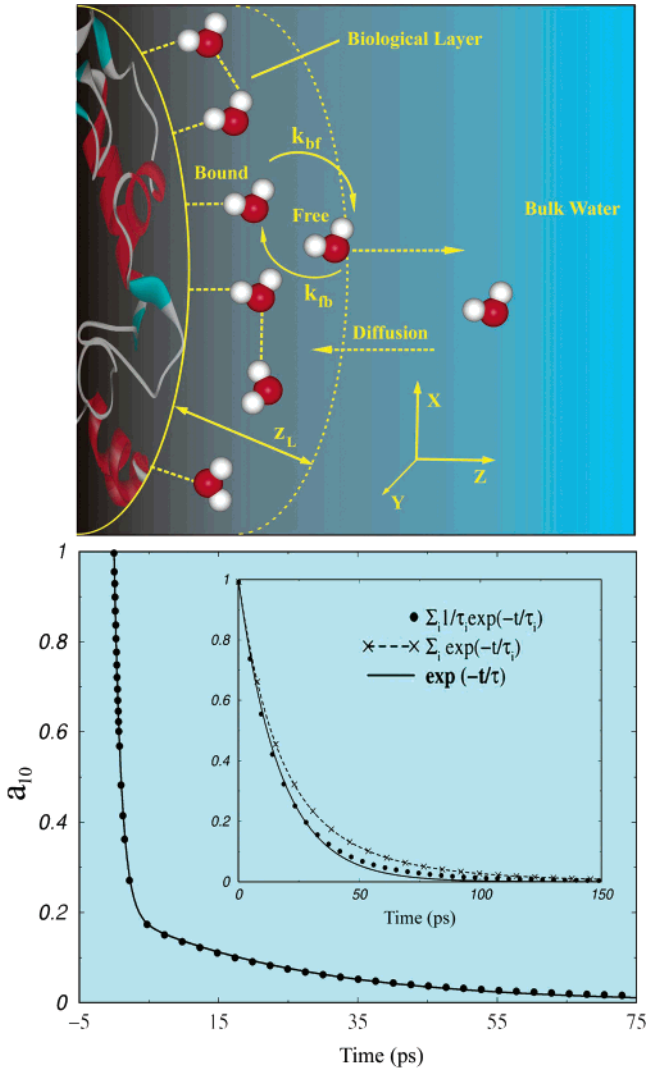

Figure 6. (Upper) Schematic of the model developed in ref 60. Hydrogen bonding of the water molecules in the layer is shown as dashed lines. There are also free water molecules that are not directly hydrogen bonded to the protein. Solid curved arrows indicate the dynamical exchange between free and bound water. Free water molecules diffuse into the layer from the bulk, and this represents a "feedback" mechanism of layer hydration. (Lower) The composite water dynamics from a heterogeneous surface layer (solid circles) fitted to a biexponential function (solid line), where $\tau_{fast} = 1$ ps (80%) and $\tau_{slow} = 26$ ps (20%). It is assumed that one-third of the sites do not bind any water molecule, and 80% of the binding sites remain occupied with bound water (the binding sites have different bound-to-free transition rates, $k_{bf} = 0.08$, 0.06, 0.04, and 0.02 ps^{-1}). Inset: Apparent single-exponential relaxation in the water dynamics from a heterogeneous surface layer. The filled circles represent the function $F_1(t) = \sum_i (1/\tau_i) \exp(-(t/\tau_i))$ plotted against time. The cross signs connected by a dashed line represent the function $F_2(t) = \sum_i \exp(-(t/\tau_i))$ plotted against time. In both cases, eight values of τ are considered, equally spread between 10 and 50 ps. The solid line is an exponential fit for F_1, with a time constant of 17.5 ps. The degree of orientation was also considered in calculating the longitudinal amplitude a_{10} (the coefficient in the expansion of probability distribution); see text and ref 60.

tion, and the influence of surface heterogeneity are treated in ref 60, and summarized in Figure 6. The theoretical time scale is consistent with the experimental findings of biphasic behavior, with the slow component in the 20−50 ps range, as will be detailed in the next section.

The residence time due to translational motion can be estimated by using the following well-known expression for translational motion:

$$\tau_{res} = z_l^2/6D_\perp \qquad (9)$$

where τ_{res} is the time taken to cross the layer, $D_\perp$ is the diffusion in the direction perpendicular to the protein surface, and z_l is the width (note the factor 6 here, not 2, because we are still in three dimensions). Thus we obtain an estimate of $\tau_{res} = 32$ ps (for $D_\perp = {}^1/_3\, D_{bulk}$) or longer; $D_{bulk} = 2.5 \times 10^{-5}$ cm^2/s[62] and $z_l = 4$ Å. In reality, the residence time is determined by the nature of the interaction with the surface, and details of the potential can be used to express the rate as a passage time. In turn, this can be used to estimate the average binding energy and the distribution of binding energies which characterize the hydrophobic and hydrophilic regions (see ref 8 for more details).

3. Bulk Hydration: Experimental

3.1. Methodology

Details are given in the original publications, and here we give a summary. All the transients were obtained by using the femtosecond-resolved fluorescence up-conversion technique (setup is shown schematically in Figure 7. Femtosecond excitation pulses (typically 200 nJ) were used. The pulse was tuned in these studies from 297 to 350 nm. The probe pulse was set at 800 nm and mixed with the fluorescence in a nonlinear crystal. The up-converted signal in the deep UV region (280−350 nm) was detected by a photomultiplier after dispersion through a double-grating monochromator. The transients were taken at the magic angle (54.7°) of the pump polarization relative to that of the probe (800 nm) and the up-conversion crystal's acceptance axis.

To construct time-resolved emission spectra (TRES) following the excitation pulse, we adopted the method of ref 63. For every sample solution, at least 10−15 fluorescence transients were measured as a function of detection wavelength across the emission spectrum. The observed fluorescence transients were fit to a function which is the convolution of the instrument response function with a sum of exponentials using a nonlinear least-squares fitting procedure (SCIENTIST software). The purpose of this fitting is to obtain the decays in an analytic form suitable for further data analysis. For each detection wavelength, the transient was normalized using the steady-state spectrum (or spectrum at very long time). The resulting time-resolved spectra were fitted with a Lognormal or Gaussian (asymmetric/symmetric) shape function to estimate the spectrum maximum, $\nu(t)$. The temporal Stokes shift is represented by the time dependence of the peak of the spectra. The shift in the chromophore's emission frequency (peak) which accompanies the solvent relaxation is then a measure of the dynamics of

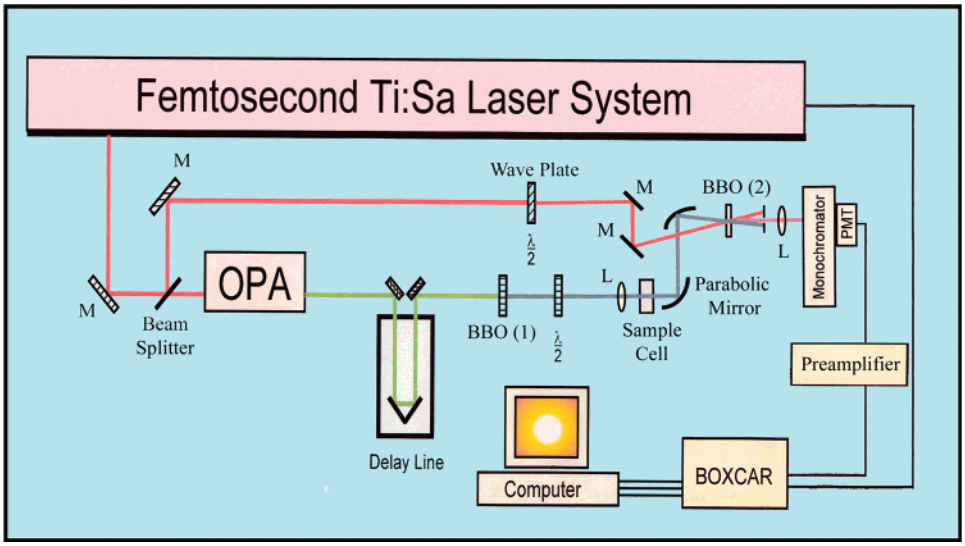

Figure 7. Schematic of the femtosecond fluorescence up-conversion experimental setup. BBO crystal (1) is used for second harmonic generation, which provides a pump beam in the UV region. BBO (2) generates the up-conversion signal of pump and probe beams. L and M indicate lenses and mirrors, respectively (see text).

solvation. From eq 1 we can define $C(t)$ in terms of observables:

$$C(t) = \frac{\bar{\nu}(t) - \bar{\nu}(\infty)}{\bar{\nu}(0) - \bar{\nu}(\infty)} \tag{11}$$

where $\bar{\nu}$ (wavenumber) is related to ν by the speed of light.

Time-resolved fluorescence studies have provided detailed experimental information about solvation.[64,65] With the femtosecond time resolution of the fluorescence up-conversion method, it has become possible to monitor solvation dynamics on the time scale of solvent relaxation; see ref 63. As noted in Figure 4, the polarization experienced at a given time is the result of the switched-on field (excited state). Note that in general we must consider the two potentials, excited and ground, and the two coordinates of the probe: intramolecular nuclear motion and that of solvation (Figure 4, upper panel and its inset). However, it is the instantaneous intramolecular Franck−Condon transition that keeps the solvent polarization (see, e.g., $P(\infty)$ in Figure 4) *the same* in both of these states and makes the energy difference between surfaces reflect the behavior of the time-dependent polarization and solvation.

To elucidate the degree of orientation (rigidity) of the probe molecule, we also study the time-resolved polarization anisotropy of emission, with femtosecond time resolution and up to the nanosecond scale. For the longer time scale, we use single photon counting techniques. In these anisotropy measurements, the pump polarization is adjusted to be parallel ($I_{||}$) or perpendicular ($I_{\perp}$) to that of the probe, defining the anisotropy as,

$$r(t) = \frac{I_{||} - I_{\perp}}{I_{||} + 2I_{\perp}} \tag{12}$$

Care was taken to ensure a high degree of polarization extinction and a relatively low power level of excitation and probing. We also have the samples in rotating cells to avoid heating and photochemical buildup of byproduct.

The preparation of samples of probe molecules, proteins, and DNA, and the biological activity measurements, are detailed in the original cited references. In all studies made, we used water from a Nanopure purification system. Buffer solutions were made from this water and buffer salts, phosphate, acetate, or tris, depending on the protein or DNA studied (the probe molecule was studied in the corresponding buffer). The concentration of the buffer salt used to maintain the pH was at most 0.1 M. The concentration of water is 55 M at room temperature.

3.2. Hydration Probes: Bulk Water

3.2.1. Tryptophan—Deciphering an Old Mystery[7,66]

Tryptophan (Trp) is the most important fluorophore (molecular structure in Figure 8) among amino acid residues for optical probing of proteins. However, Trp fluorescence is complex because of the different rotamers in the ground state and the existence of two nearly degenerate electronic states (^1L_a, ^1L_b) with perpendicular transition moments. In the past, these two issues contributed to some confusion. In what follows we summarize the new results which make it possible to study solvation on the ~1 ps time scale.

The fluorescence of tryptophan in water shows nanosecond and picosecond decays. The nanosecond decay has been previously reconciled with the presence of two conformers (studied by NMR[67]) with unique decay times of ~0.5 and 3.1 ns.[68] The pre-exponentials of these two components depend on the emission wavelength. The study constructed nanosecond time-resolved spectra of tryptophan in water for the two components and obtained maxima of the peaks of the two species at their earliest time (t = 0); the spectrum of the short-lived (~0.5 ns) component gave a maximum at 335 nm, while that of the 3.1 ns component was located at 350 nm, the usual

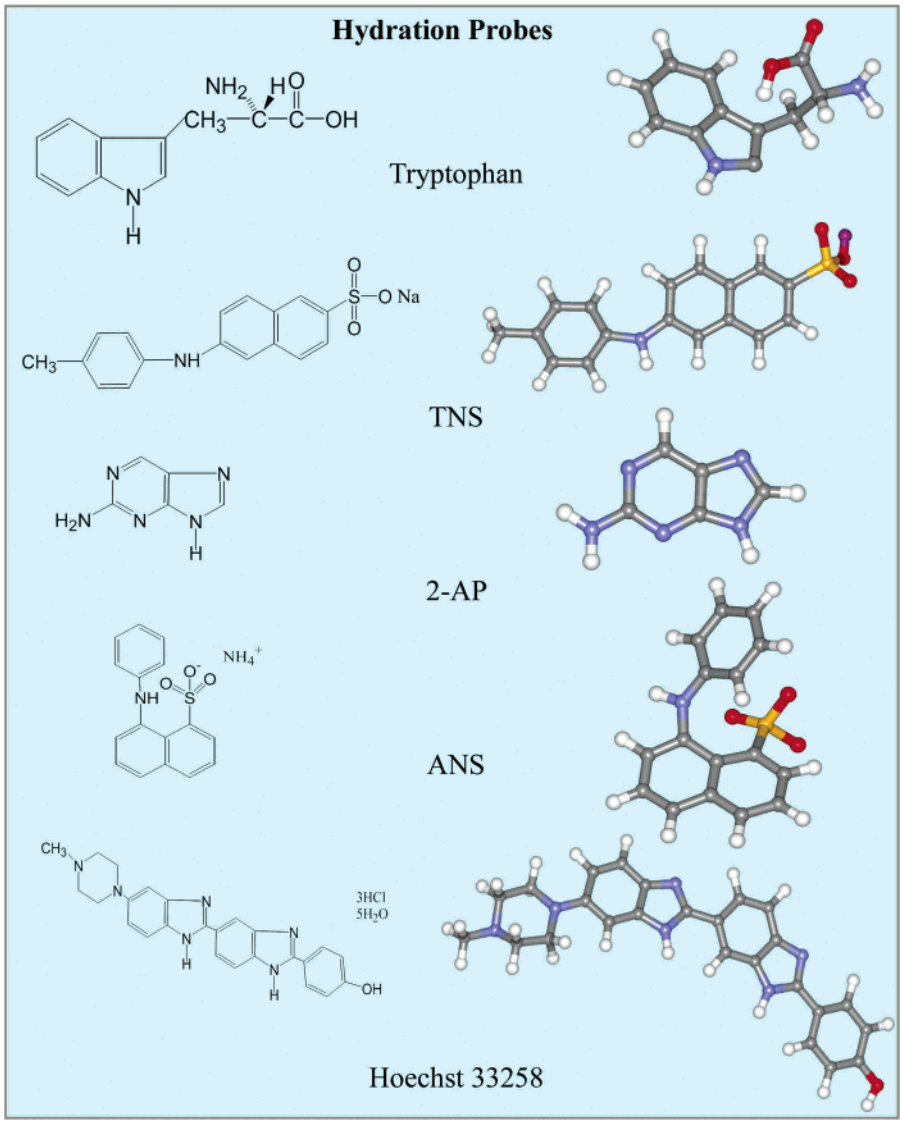

Figure 8. Molecular structures of the hydration probes used in our studies.

steady-state maximum recorded for aqueous tryptophan. Accordingly, in studies of solvation on the time scale of ~1 ps, one should not normalize to the steady-state spectrum but instead should use the spectrum at times much longer than solvation but much shorter than those which characterize the nanosecond rotamer change; Shen and Knutson[69] and we[7] used 20 ps. In this way we can separate the effect of conformational heterogeneity from that of solvent relaxation times (~1 ps) in bulk water. The time scale observed in the protein hydration dynamics using tryptophan as a probe is in the range of 20−50 ps, which is also much faster than the expected nanosecond conformational relaxation dynamics. However, in proteins the time-integrated spectrum shifts to the blue (see below), and the evolution of the spectra is nearly complete in less than 200 ps.

The indole chromophore of tryptophan possesses overlapped ^1L_a and ^1L_b absorption dipoles,[70] and the "level crossing kinetics" between these nearly perpendicular transitions exerts a large influence on the anisotropy. Because of the orthogonal dipoles of the two states, anisotropy measurements should probe the interconversion between them. Time-resolved experiments (cross correlation 500 fs) by Ruggiero et al.[71] gave an anisotropy decay (excitation at 300 nm and emission at 330 ± 5 nm) of 1.2 ps, which they attributed to this process of internal conversion of ^1L_b to ^1L_a. They pointed out the potential dangers of likely level crossing entanglement for the anisotropy and detected the solvent relaxation (~1 ps) of water around tryptophan as a probe. However, recent works from this laboratory[7,66] and by Shen and Knutson[69] showed that the anisotropy decays in 100 fs or less, indicating that the conversion is much faster than the solvent relaxation time (~1 ps). A potential reason for the discrepancy between the measurements by Ruggiero et al.[71] and those reported in refs 7, 66, and 69 might be distortion by Raman scattering, since many of the wavelengths which showed a large amplitude of the 1.2 ps "anisotropy" component register with expected wavelengths for Raman scattering. The Raman scattering peak for the excitation wavelength at 300 nm would be at 333.9 nm; control experiments at 295 nm excitation and 325 nm emission confirmed such a contribution.[69]

This separation of time scales is further supported by the wavelength dependence of absorption and

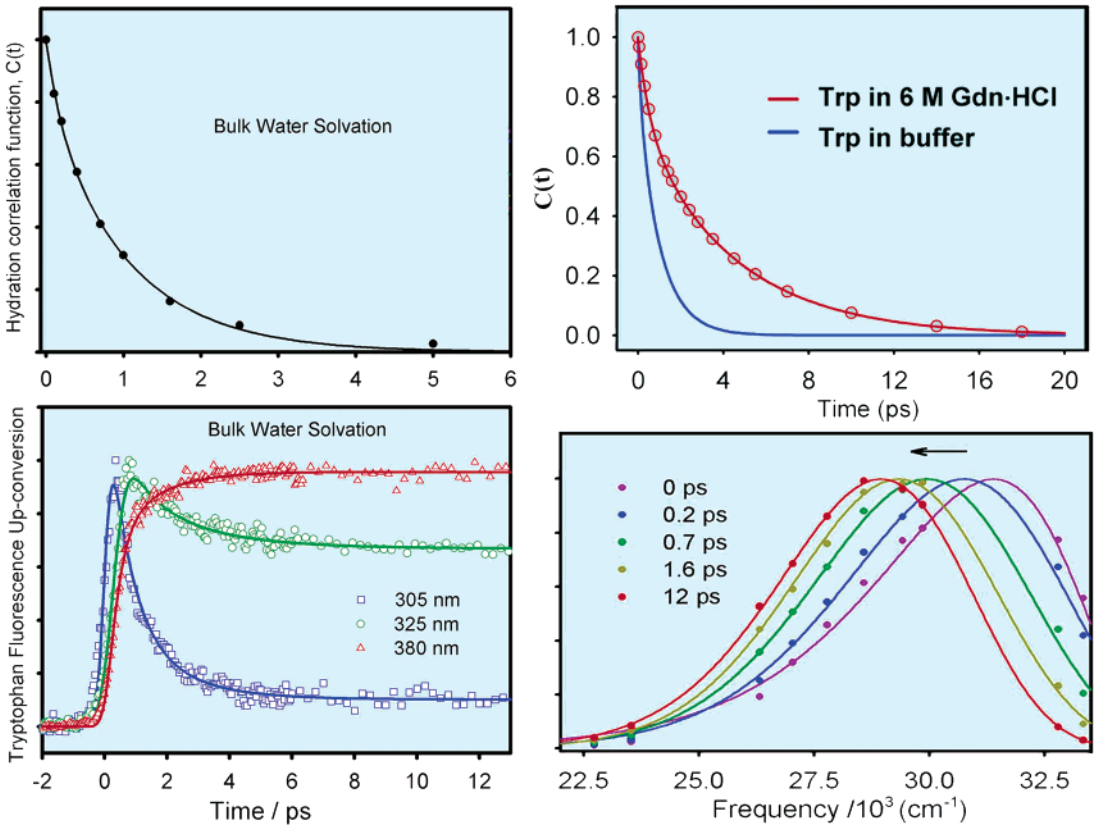

Figure 9. Femtosecond-resolved fluorescence (lower, left panel), and the normalized spectral evolution at five delay times from $t = 0$ (lower right panel) for tryptophan in bulk water. The excitation wavelength was 288 nm. In the upper left panel we give the hydration correlation function. The correlation functions for Trp in aqueous buffer and 6 M Gdn·HCl solutions are shown in the upper right panel. The evolution from the nonequilibrium to the equilibrium state of solvation is evident, and the time scales are indicated.

anisotropy measurements. The relative absorption strength of the two states at various excitation wavelengths can be estimated by measuring the initial anisotropy, r_0. The excitation wavelength-dependent anisotropy study clearly indicates[69] that at shorter wavelengths (e.g., ~290 nm) the mixing is 50%, while at longer wavelengths (e.g., ~300 nm) the ^1L_a absorption dominates. We used the excitation wavelength at 296−297 nm for the studies of protein hydration, using tryptophan as a probe, and the absorption strength of the ^1L_a state is close to 95%; our initial anisotropy of ~0.25 further supports this dominance. We therefore are able to separate solvation dynamics (~1 ps or longer) from the interconversion (~100 fs or less) and as such make tryptophan a powerful probe of hydration in native proteins.

Fluorescence up-conversion scans of aqueous Trp solutions are presented in Figure 9. The excitation wavelength for this experiment was 288 nm. As indicated in previous publications from this group and another group,[66,69] the ultrafast decays observed on the blue side of the spectrum, and the corresponding rises in the red edge, reflect a dynamic spectral shift which is a signature of relaxation of the solvent around the large dipole of the fluorescing state of Trp: ^1L_a.

In bulk water, the Trp solvation $C(t)$ curve can be fitted to a biphasic decay, the sum of two exponential decays: $\tau_1 = 180$ fs (20%) and $\tau_2 = 1.1$ ps (80%). This dynamic Stokes shift behavior is typical of solvation of a molecular probe in bulk water, and the time scale[7] is consistent with our previous study of Trp at pH 2, with excitation at 266 nm.[66] The ultrafast behavior of the $C(t)$ curve in this case corresponds to relaxation of the water molecules involving both inertial (sub-100 fs) and diffusive (overdamped) rotational motions (up to ~1 ps).[49] Rotational motions of the solvent molecules dominate the relaxation trajectories, and the contribution from the translational motion is small. The inertial part of the response is due to pairwise solute−solvent interactions, while for the diffusive part more collective motions of the solvent molecules are present.[54]

We also studied tryptophan in concentrated salt (denaturant) solution. We constructed the hydration correlation function for Trp in 6 M GndHCl following the same methodology described above. These results are presented in Figure 9. The hydration correlation function for the Trp/6 M GndHCl solution shows a biexponential decay with $\tau_1 = 570$ fs (28%) and $\tau_2 = 4.4$ ps (72%). These time constants are significantly longer than those observed for Trp in buffer solution without the denaturant ($\tau_1 = 180$ fs (20%) and $\tau_2 = 1.1$ ps (80%)). The change indicates that the presence of $GndH^+$ and Cl^- ions significantly slows the solvation dynamics, and the effect must be taken into account when considering the dynamics of a probe in concentrated salt solutions. We shall return to this point later.

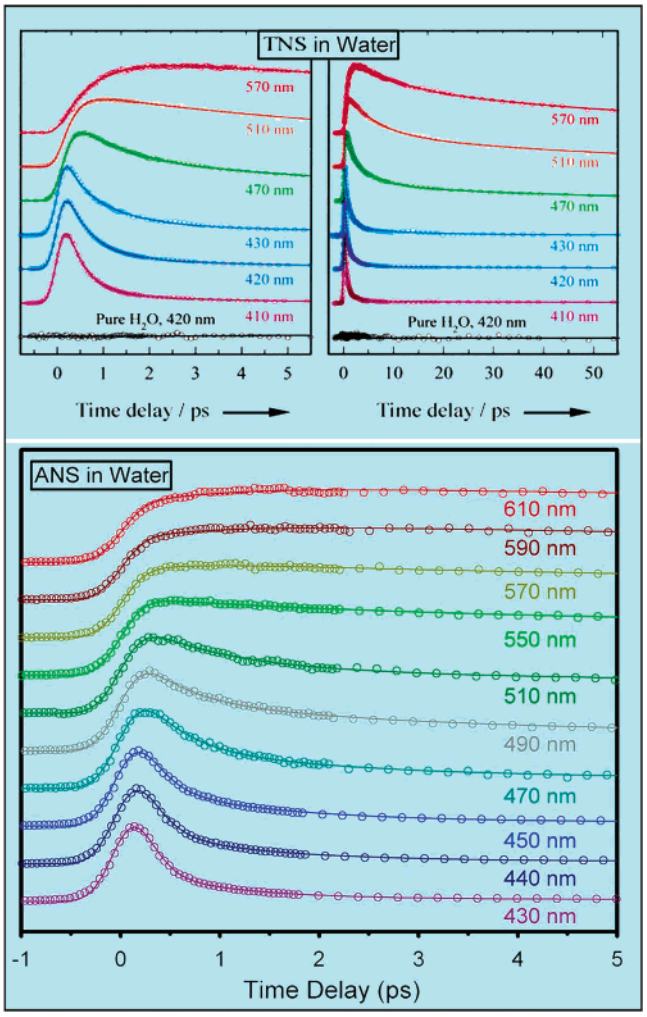

Figure 10. (Upper) Femtosecond-resolved transients of TNS in bulk water with a series of wavelength detection shown for short (left) and long (right) time scales. Transients are normalized for comparison. The pure solvent signal, without the probe, is shown here for water at 420 nm. (Lower) Femtosecond-resolved fluorescence at a series of wavelengths for ANS in water. The excitation wavelength was 320 nm.

3.2.2. 2-(p-Toluidino)naphthalene-6-sulfonate in Bulk Water[72]

2-(*p*-Toluidino)naphthalene-6-sulfonate (TNS, molecular structure in Figure 8) is a biologically common fluorescent probe. The emission of the probe (quantum yield and fluorescence maximum) is very sensitive to the local environment. For example, the emission of TNS in bulk water has a quantum yield of ~0.001, and when we measured it in CTAB micelles (nonpolar medium) we found that the fluorescence emission increases ~670 times. The maximum shifts to the blue by 40 nm, from 470 nm in bulk water to 430 nm in the micelle (325 nm excitation); see ref 72.

The upper panel of Figure 10 shows the femtosecond-resolved transients of TNS in pure water with a systematic series of wavelength detection. All transients show three distinct time scales. The signal initially decays at the blue side (410−470 nm) in 390−770 fs but rises at the red side (470−570 nm) in 190−680 fs. In contrast, on the picosecond time scale, the second component decays for all wavelengths detected with time constants of 1.9 (410 nm), 2.6 (420 nm), 3.2 (430 nm), 3.8 (470 nm), 5.8 (510 nm), and 10 ps (570 nm). The long-time component decays with a time constant of ~60 ps.

The initial femtosecond decay at the blue side and rise at the red side is a manifestation of solvation dynamics in water. We constructed the correlation function, $C(t)$, and obtained a solvation time of ~700 fs, consistent with the reported value for bulk water.[49,51] It should be noted that the $C(t)$ for coumarin 343 reported in ref 49 has an initial Gaussian-type component (frequency 38.5 ps^{-1}, ~25 fs, 48% of total amplitude) and two exponential decay components of 126 (20%) and 880 fs (35%). Our solvation here is concerned with up to 1 ps decay without resolving the initial ~100 fs component. Accordingly, the blue and red sides of the emission, which have similar dynamical time scales, reflect the diffusive (~800 fs) motion of water molecules. Longer decay of solvation is not resolved because of the competing intramolecular charge transfer (CT) process which is discussed in detail elsewhere[72] and shown in Figure 10. The observed picosecond component, which is always manifested as a decay, represents the twisting motion of TNS in a barrier-crossing from the initial to the final state of charge separation.

3.2.3. 1-Anilinonaphthalene-8-sulfonate in Bulk Water[10]

1-Anilinonaphthalene-8-sulfonate (ANS, molecular structure in Figure 8) is also a well-known solvation probe.[73,74] The steady-state fluorescence spectra show a large red solvatochromic effect: the fluorescence maximum changes from 390 nm in *n*-hexane to 490 nm in methanol, and to 540 nm in aqueous solution (buffer, pH 3.6 and 6.7).[10] The steady-state emission is quenched dramatically in polar solvents. Because of its bichromophoric structure, ANS is known[75] to undergo CT from one aromatic moiety to the other ring and solvation. In the steady state, in nonpolar solvents, the emission is strong and is mostly from the locally excited state, i.e., prior to charge separation. In polar solvents, the fluorescence decreases and is dominated by emission from the CT state. The solvent polarity and rigidity determine the wavelength and yield of emission, and that is why ANS is a useful biological probe.

Time-resolved emission separates the contribution of ultrafast solvation from longer-time, nonradiative processes. As shown in the lower panel of Figure 10, the femtosecond transients are typical of those observed for other chromophores in water. On the blue edge of the spectrum, the signal is seen to decay on the time scale up to ~1.5 ps, while on the red edge it rises on a similar time scale. From this family of transients we constructed the $C(t)$ in Figure 11, $\nu(t = \infty)$ at 5 ps; $C(t)$ shows two exponential decays of 185 fs (22%) and 1.2 ps (78%), indicating that hydration is complete on this time scale, as is the case with other solutes, including coumarin dyes[49,51] and tryptophan.[7]

On longer time scales, all transients at different wavelengths have a contribution (up to ~10%) which decays with a time constant of 5−10 ps, depending

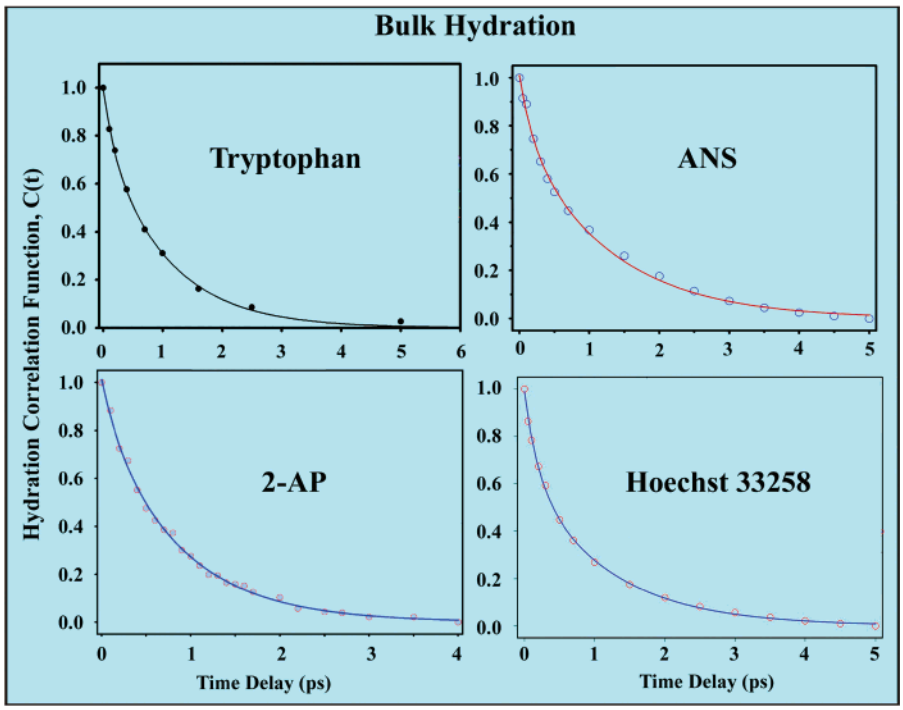

Figure 11. Hydration correlation functions of bulk water using the different molecular probes indicated. Note the similarity in behavior.

on wavelength, and is then followed by a decay to the baseline with a time constant of 150−300 ps, depending on the wavelength. This subnanosecond decay is the lifetime of ANS in water; we confirmed this by measuring the lifetime in water and methanol using single photon counting techniques and obtained values of 0.25 and 5 ns, respectively. These decays describe the nonradiative pathways from the locally excited state to the CT state and the total lifetime of the latter in water, as detailed in ref 10.

3.2.4. 2-Aminopurine in Water[76]

The analogue of adenine, 2-aminopurine (2-AP, molecular structure in Figure 8), is commonly used as a fluorescent sensor base, and in this laboratory we have used it as a probe for studies of electron transfer in DNA duplexes and with nucleotide (see below). 2AP is structurally similar to the natural base adenine (A), with almost the same properties of base pairing with thymine[77] and even cytosine.[78] 2-AP in bulk water has an absorption maximum at 304 nm. From the steady-state spectra, the solvatochromic shift of the fluorescence toward longer wavelengths with an increase in solvent polarity is evident; see ref 76.

The transients for different wavelengths, from the blue to the red side of the fluorescence spectrum of 2-AP in water, have been studied.[76] The emission transients detected in the blue region of the fluorescence spectrum are characterized by an instant rise (cross-correlation) and typically a picosecond decay component. When detection is made in the red region, the decay part slows until eventually an initial rise on a picosecond time scale is observed. The lifetime of 2-AP in the relaxed equilibrium state is 11.8 ns.[79] These overall features are well recognized as being characteristic of solvation dynamics.

The time evolution of $C(t)$ is shown in Figure 11. The decay of $C(t)$ was fitted to a biexponential function, giving two time constants of ∼200 (15%) and 870 fs (85%); the ∼50 fs or less component was not resolved. The net dynamical spectral shift is 610 cm^{-1}, from 27 140 to 26 530 cm^{-1} (4 ps). The temporal behavior of the $C(t)$ is similar to that of tryptophan as a solvation probe.[7] This is consistent with the fact that both probes interrogate the same dynamics of bulk water; both increase their dipole moments upon excitation: for tryptophan it is ∼6 D, while for 2-AP the increase is estimated to be $1.6 \leq \Delta\mu \leq 2.9$ D.[80] It should be mentioned that 2-AP is used extensively in studies of electron transfer, and the separation of time scales for solvation and electron transfer becomes important in such donor−acceptor complexes involving 2-AP.

3.2.5. Drug Hoechst 33258 in Bulk Water[11]

The drug Hoechst 33258 (H33258, molecular structure in Figure 8), which is in a class of antimicrobial agents,[81] has high affinity to DNA ($K_d \approx 10^{-8}$ M); its fluorescence intensity increases when it is complexed to DNA, relative to that in aqueous solution, and is accompanied by a significant blue shift.[82−84] The steady-state fluorescence spectra show a large red solvatochromic effect; see ref 11. The fluorescence maximum changes from 436 nm in dioxane to 477 nm in ethanol and to 510 nm in aqueous buffer solutions.

Femtosecond-resolved fluorescence up-conversion transients of the drug in bulk water (buffer) have been studied for at least 13 of these transients at different wavelengths. The femtosecond transients are typical of those observed for the other chromophores discussed above. On the blue edge of the spectrum the signal is seen to decay (∼1.5 ps),

whereas on the red edge it rises on a similar time scale. The signal ultimately decays to the baseline on a much longer time scale, with time constants of ~40 and 500 ps. From the transients, it is clear that the contribution of ultrafast hydration is well separated from the nonradiative processes. Two major processes[84,85] are involved in the deactivation of the excited state, as discussed in ref 11.

The constructed $C(t)$ shows (Figure 11) the biphasic behavior, an apparent biexponential decay with time constants of 195 fs (33%) and 1.2 ps (67%). The overall spectral shift we observed is 3184 cm^{-1}; any sub-100 fs component in the dynamics would be unresolved. To complete the picture regarding bulk dynamics of the drug in water and in a less polar solvent (for comparison with the DNA environment), we made similar studies of the drug in ethanol (data not shown). In this case, decays are slower than those in water and consistently show the time scale of solvation for ethanol (the average solvation time is 16 ps[63]). In water, the fluorescence is quenched dramatically; the quantum yield is 0.015 in water and increases to 0.5 in ethanol.[83]

In conclusion, all probes studied (tryptophan, TNS, ANS, 2-AP, and H33258) show characteristics of solvation dynamics in water with a biphasic behavior but up to ~1 ps decay. The variation on this time scale for the different probes (e.g., 0.8 vs 1.1 ps) reflects the additional specific interaction with the solvent, e.g., through hydrogen bonding; there is also the effect of changes either on the probe (TNS and ANS are salts) or added salts to the bulk, as discussed below. It has been shown[86] that solvation times of different solute molecules—16 of them—in the same solvent (1-propanol) can vary somewhat because of the specific interactions, but the change is relatively small, in our case ~20%. For all the probes studied in this laboratory, the dynamics on longer time scales are absent (tryptophan and 2-AP) or present (TNS, ANS, and H33258); 2-AP in DNA or with other nucleotides becomes involved in electron transfer. The lifetimes of these probes are on the subnanosecond to nanosecond time scales. The hydration correlation functions of these probes (Figure 11) show the similarity in behavior for bulk water on the time scale of ~1 ps.

Elsewhere[10,76] we have considered the time scale and influence of vibrational relaxation. For the probes used in our studies, we found a relatively insignificant role of vibrational relaxation/redistribution, consistent with previous work.[63] In these large molecules, these relaxations may occur on the subpicosecond time scale,[87] but this will be true for excitation with significant internal energy, which is not the case in our studies. For example, the absorption spectrum of ANS in water cuts the emission spectrum in *n*-hexane (gas-phase-type emission) at 373 nm, indicating a putative 0−0 transition close to the excitation wavelength at 320 nm. Thus, solvation red shift (~7000 cm^{-1}) is dominant over the intramolecular Stokes shift. This dominance of solvation was confirmed by studies of two probes (tryptophan and 2-aminopurine) at low and high vibrational energy.[7,66,76] These observations are further supported by the fact that the shapes of TRES at early times are not significantly different from those obtained at later times, and that the ANS transients in different solvents (water, methanol, and ethanol) give the characteristic solvation times obtained using other probes. It should be noted that, in the study of the protein α-chymotrypsin, the effect of the pH was observed under identical conditions of excitation and relaxation, and the changes observed are consistent with the vibrational relaxation being insignificant.

4. Proteins: Hydration and Function

4.1. The Enzyme Subtilisin *Carlsberg*[7]

The protein is in a class of endopeptidase which hydrolyze the peptide bond away from the termini of a substrate polypeptide chain. We use the *single* tryptophan (Trp) residue (Trp113) in the enzyme (serine endopeptidase) subtilisin *Carlsberg* (SC) as an intrinsic fluorescent probe. The single indole side chain of SC at Trp113 is on the surface of the protein and is significantly exposed to the water environment (see Figure 12 for the crystal structure of SC). The main advantage of using Trp to study the local molecular dynamics of the protein surface is that its intrinsic nature rules out any ambiguity about the location of the probe and about the heterogeneity at different sites. While the ground state of Trp has a very small dipole moment, a hydrophobic residue, the electronically excited ^1L_a state has a large static dipole, and it is the emitting state in water (see previous section). The energy gap to the electronic ground state is very sensitive to the local environment, and the spectral shift follows the polarity of the medium, including proteins;[88] in polar media, the spectrum shifts to the red. In the SC protein, the Trp residue resides in a site that is significantly exposed to water. Thus, we are able, upon UV excitation, to follow its solvation in the dynamic Stokes shift, caused by water relaxation on the femtosecond to picosecond time scale. We then compare with the results obtained for free Trp in bulk water.

The hydration dynamics (Figure 12) of the SC protein show important differences when compared with the results of Trp in bulk water. In particular, the $C(t)$ shows the biphasic behavior but with a considerably slower decay component; it is described by the sum of two exponentials, with $\tau_1 = 800$ fs (61%) and $\tau_2 = 38$ ps (39%), much different from the observation made in bulk water. The overall spectral shift we observed is 1440 cm^{-1}: $\nu_{max}(0) = 30\,710$ cm^{-1}, $\nu_{max}(200\text{ ps}) = 29\,270$ cm^{-1}. Clearly, the local protein environment of the indole chromophore at the surface of SC changes the dynamics from that of tryptophan in bulk water.

The anisotropy $r(t)$ decays with a time constant of 55 ps (50%) and then remains constant at least up to 200 ps. For tryptophan in bulk water, this anisotropy, after the femtosecond component (previous section), decays to zero with a time constant of 35 ps. This 35 ps decay is the rotational relaxation of a free molecule in the bulk solution. In the protein, the behavior of the anisotropy suggests that the rotational reorientation of the probe (and the protein)

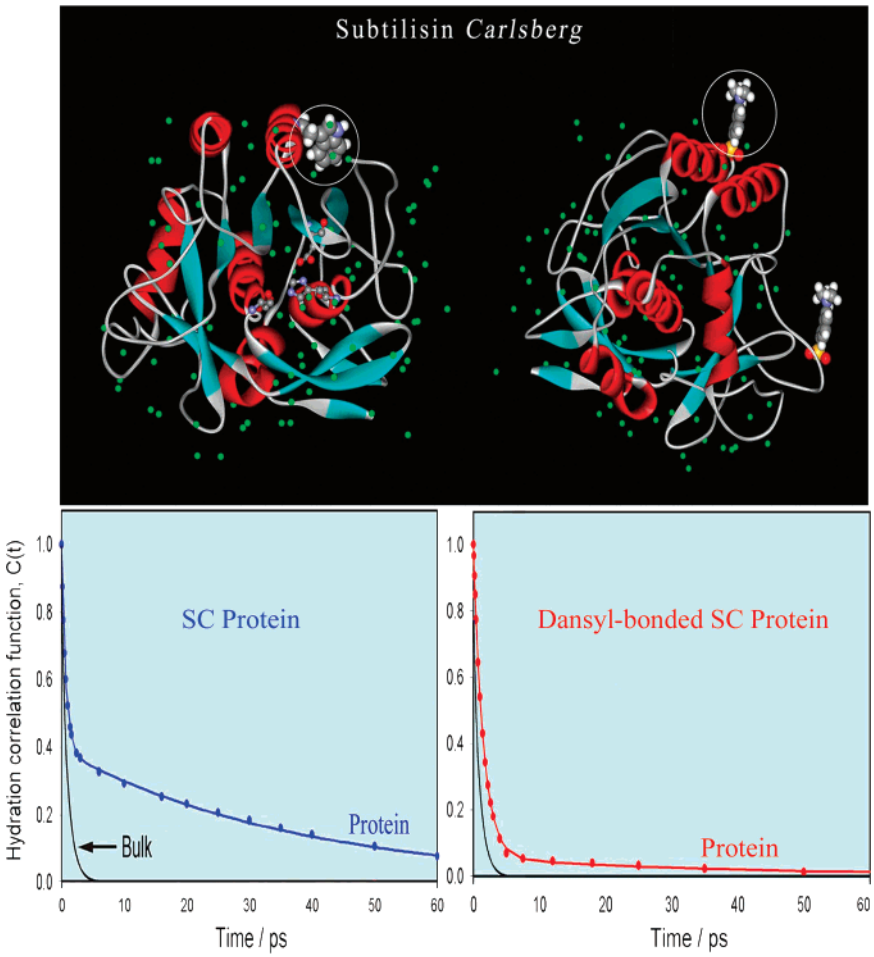

Figure 12. (Upper left) High-resolution X-ray structure of the protein subtilisin *Carlsberg*. This structure was downloaded from the Protein Data Bank and processed with WEBLAB−VIEWERLITE. We depict the position of the single Trp residue of the protein. Note the bound water molecules around this residue. (Upper right) Two of the nine potential binding sites (Lys and Arg residues) for dansyl chloride labeling. (Lower) Hydration correlation function obtained from femtosecond fluorescence up-conversion measurements of aqueous solutions of the subtilisin *Carlsberg* protein (left) and dansyl-labeled subtilisin *Carlsberg* (right). For comparison with Trp in bulk water we show the $C(t)$.

occurs on a much longer time scale; the 50 ps decay is accordingly a reflection of the fluctuation of the indole chromophore orientation when anchored in the protein backbone.

To examine the distance dependence, we made another set of femtosecond studies of hydration for a covalently attached dansyl chromophore. This labeling is well known[89] to occur at the ϵ-amino groups of the lysine and arginine residues, which are water-exposed. There are nine such sites in SC. Two of these binding sites are depicted in the Figure 12. On the basis of bond lengths, we estimate that the location (∼7 Å) of the dansyl probe, when bound to SC, is such that it sees relatively smaller interaction with the protein backbone and side chains in comparison with bulk water. The dansyl chromophore undergoes a twisted intramolecular charge transfer in the excited state to generate the fluorescing state,[90] and the process of solvation leads to continuous red shift of the emission spectrum, similar to the behavior of TNS.[72] As shown in Figure 12, the hydration correlation function $C(t)$ decays much differently from that of Trp in the native SC. Here, the $C(t)$ function has an ultrafast decay with a time constant of 1.5 ps (94%), and only a very small amount of spectral shift occurs, with a time constant of 40 ps (6%). The total shift is 1180 cm^{-1}: $\nu_{max}(0) = 21\,430$ cm^{-1}, $\nu_{max}(200$ ps$) = 20\,250$ cm^{-1}. The near absence of the ∼40 ps decay indicates that, at a separation of ∼7 Å from the surface, the solvent dynamics resemble, to a large extent, those seen in bulk water.

The study is, to our knowledge, the first characterization of the ultrafast dynamics of solvation at the surface of a protein using a *single* native Trp residue. Thus, it probes water dynamics at the interface without spatial averaging or the position inhomogeneity of an extrinsic probe. Two types of trajectories of solvation have been observed, bulk type and protein layer type, and both are dynamically involved and reflect the distribution in the residence times at the local surface site of the protein. The time scales observed in the apparent "bimodal" behavior of the hydration correlation function determine the local order and rigidity. The probe itself is relatively rigid, restricted in motion in the protein, as evidenced by its anisotropy decay, but the water reorientation in the network is what determines the rigidity of the layer. By about 7 Å, essentially all of the water is bulk type. The biphasic behavior is consistent with the theoretical description given in section 2. The femtosecond component suggests the presence of labile water in the layer, while the residence time of

bound water in the layer is reflected in the 38 ps component (k_{bf}^{-1}). Using eq 9, and assuming the dominance of translational diffusion, we can estimate the layer thickness for a 38 ps time as ~5 Å.

The significance of these findings to the biological function of the enzyme protein SC may now be considered. The enzymatic activity of the protein, which involves the hydrolysis of a peptide bond, away from the termini of a substrate polypeptide chain, is a surface function. It depends on the efficiency of recognition of negatively charged and polar amino acids of the substrate peptide.[91] The bulklike environment in the close vicinity of the surface would enhance the interaction with the substrate. On the other hand, the structured water molecules are needed around the protein surface to be part of the chemistry and possibly maintain a 3D structure. Thus, the time scale for hydration and exchange dynamics is crucial to the tradeoff between the structure and its enzymatic function, and the bimodal behavior reported here could be of fundamental importance for such function.

4.2. The Protein Monellin[9]

This protein monellin, which like SC contains a single water-exposed Trp, is a sweet-tasting protein originally isolated from the berries of the plant *Dioscoreophyllum cumminsii*.[92,93] On a molar basis, the protein is about 50 000 times sweeter than sucrose and has been the subject of numerous studies aimed at understanding the mechanism of taste.[94,95] Here we report observations made on monellin, in both its native and denatured states. For the native state, we found that the picture of dynamically ordered water is robust, but the exchange with the bulk has a different time scale, 16 ps instead of 38 ps for SC; the bulk-type hydration occurs in 1.3 ps.

Monellin consists of two polypeptide chains associated by interchain hydrogen bonding and hydrophobic interactions.[96,97] Chain A contains 45 residues, and chain B has 50 residues, including a single Trp at position 3 from the N-terminal. Although the crystal structure from the Protein Data Bank (4MON) shows monellin as a dimer, the characterization of the protein by electrophoresis and gel filtration showed that it exists as a monomer in solution.[93] Further indication that monellin is a monomer comes from comparisons with the protein single-chain monellin (SCM), which has been shown to be in the monomer state by NMR;[98] SCM is an analogue of monellin engineered by fusing the two chains in monellin. The X-ray structure of the protein monomer is shown in Figure 13.

The biphasic $C(t)$ function gives two time constants, 1.3 (46%) and 16 ps (54%); any sub-100 fs components in these dynamics are unresolved. The net spectral shift observed is 960 cm^{-1}. In Figure 13, we present the solvent response function obtained for free Trp in the buffer and that of the protein. Clearly, the hydration dynamics for the Trp site at the surface of monellin are significantly different from those in bulk water. The results of the anisotropy measurements indicate that hydration dynamics in monellin occurs for a probe which is "restricted" in its motion.[9] Like

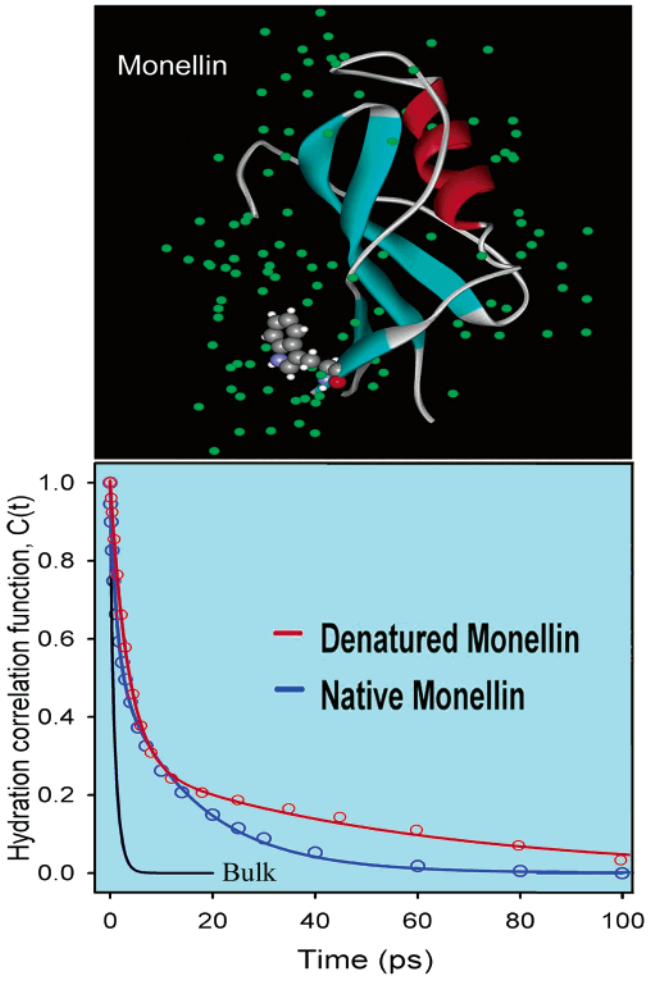

Figure 13. (Upper) X-ray crystal structure of the protein monellin. The structure was downloaded from the Protein Data Bank (4MON) and processed with the program WEBLAB−VIEWERLITE to show only one of the monomers. In solution, monellin exists as a monomer.[93,98] (Lower) The hydration correlation function $C(t)$ for monellin. The hydration correlation functions obtained for free Trp in the same buffer and for denatured monellin are also shown for comparison (see text).

in the case of subtilisin *Carlsberg*, the slow hydration mode, due to bound water molecules, is related to the rate of transition from bound to free states: $\tau_{slow} \approx k_{bf}^{-1}$ (see above). For the proteins monellin and subtilisin *Carlsberg*, these τ_{slow} values are observed to be 16 and 38 ps, respectively. The effective binding energy determining the respective residence time is estimated to be, at minimum, 1.2 kcal/mol for monellin and 2.3 kcal/mol for subtilisin *Carlsberg*, taking the potential energy function for the transition from the bound to the free state to be a double Morse potential. Details of the potential and the calculations are included in ref 8. MD simulations on these proteins will elucidate details of the dynamics.

To study how dynamics depend on the presence of a well-defined landscape of hydration sites near the Trp residue, we have studied monellin in its denatured state. The steady-state emission results for a solution of monellin in 6 M GndHCl show a shift from 342 to 352 nm, indicative of denaturation. At such a GndHCl concentration, monellin can be considered to exist as statistical random coils.[99] From the density

of the 6 M GndHCl solution, we calculate that there is approximately one $GndH^+$ or Cl^- ion for every three water molecules. To establish how such a large concentration of ions alters solvation in the bulk, as discussed above, we have also studied the dynamics of free Trp in solution of the same concentration (Figure 9).

The $C(t)$ function for denatured monellin in Figure 13 can be fitted to a biexponential decay with $\tau_1 = 3.5$ ps (72%) and $\tau_2 = 56$ ps (28%). The time constant of the first part of the dynamics (3.5 ps) is increased from the value of 1.3 ps in native monellin. Also, the contribution of the fast component to the total spectral shift significantly increases from 46% to 72%. The solvation dynamics of Trp in the 6 M GndHCl solution occurs on a time scale similar to that of the fast component in denatured monellin. From this comparison, we conclude that the 3.5 ps component is due to bulk-type solvation around the Trp site in the random coil/6 M GndHCl. It is important to note that the ~16 ps component seen in native monellin is completely absent, indicating that, in the denatured state, the dynamically ordered hydration layer is indeed disrupted.

Solvation of the Trp/6 M GndHCl is significantly faster than the 56 ps decay observed for denatured monellin. This much slower decay must be inhomogeneous due to "solvation" by ions and water molecules in collapsed pockets and/or due to the relaxation of the coiled protein structure around the Trp moiety. In the denatured protein, we expect a large degree of inhomogeneity, which most likely will produce multiple solvation times; therefore, the 56 ps time scale should be taken as an average time which might include even slower components outside our time window. It should be noted that such inhomogeneity is also reflected in parts of the spectrum which exhibit different probe lifetimes.

A simple model was advanced in ref 8, which accounts for solvation energy fluctuations that are coupled to the dynamics of a random polymer chain. The model considers the chain's solvation energy time correlation function to behave as a multiexponential, with decay times given by Rouse chain-type homopolymer dynamics. The eigenvalues associated with the chain's normal modes yield time scales that range from ~10 ps to ~30 ns for a polymer similar in length to chain B in monellin (50 units). The 56 ps component would be a signature of these fluctuations in the time window (200 ps) scanned. The implication is that the hydration of Trp is directly or indirectly, through its degree of bulk exposure, controlled by the fluctuations of the structure of the random coil. However, any model must consider the high concentration of surrounding ions.[100,101] In ref 60, we considered the effect of salt on the hydrogen bonding and on the reduction of the diffusion coefficients for both translation and rotation as a results of the increased friction due to the presence of ions.

The dynamical picture of hydration presented for monellin is relevant to the function of the protein, given the time scale and the form of the response. One of the primary processes in monellin taste function is the recognition of another protein, namely a G-protein complex. In this process, desolvation is controlled by the time scale of water in the layer. It is now clear that, if this time is shorter than the time for diffusion of the protein, such dynamics make possible an efficient recognition, but with the maintenance of the globular structure.

4.3. The Enzyme α-Chymotrypsin[10]

The protein α-chymotrypsin (CHT), isolated from bovine pancreas, is in a class of digestive enzymes and has the biological function to hydrolyze polypeptide chains. However, physiological activity is determined by the pH. Here, our interest is in the possibility of relating protein hydration to the expression of functionality. For this reason, we examined the local hydration dynamics at the surface of CHT. The fluorescence of the probe ANS (see section 3.2.3), commonly used to monitor structural changes of proteins and membranes, was studied with femtosecond resolution in two states of the protein, the physiologically *active* and *inactive* states.

The enzyme is not active at lower pH, but the activity increases nonmonotonically with pH[102]—in the duodenum, with low pH, it is inactive, while in the lower small intestinal track, with high pH, it becomes active.[102,103] The inactivity of the enzyme at lower pH is known to be related to the protonation of the residues of the catalytic triad.[102] The crystal structure (Figure 14), as discussed below, gives the active site for the enzyme and the site for recognition of ANS, which is unchanged at both pH ranges;[104,105] from spectroscopic studies, it was suggested that the degree of mobility of water molecules, not the hydrophobicity, may be the important factor for the change with pH.

Such a change in activity of the protein with pH offers a unique opportunity for correlating the function with the dynamics, since the global structure and binding site for recognition are unchanged in either pH range. By careful study of the hydration of the protein surface at different pHs, and of ANS in bulk solvents (water, methanol, ethanol, and *n*-hexane), we are able to relate expressions of functionality to the order and rigidity of the hydration shell and determine the rate at which hydration occurs, from the femtosecond to the picosecond scale.

The $C(t)$ functions constructed from femtosecond-resolved transients are shown in Figure 14. The functional decays give the following results for pH 3.6: 290 fs (40%), 2.9 ps (10%), and 43 ps (50%). For pH 6.7, we obtained 260 fs (51%), 1.8 ps (39%), and 28 ps (10%). Clearly, for the ANS−protein complexes, we observe the slow component characteristic of hydration with a significant contribution, and the time scale is 2 orders of magnitude different from that for bulk-type solvation. Moreover, the ultrafast decay is dominant in the high-pH case. From the equilibrium constant, we know that ~15% of ANS is free in the buffer and will contribute only to the ultrafast part of the decay. However, the trend observed for the increase in the amplitude of the ultrafast component with pH cannot be from the free ANS molecules because K_{eq} is nearly the same at the two pH values. In fact, it is somewhat larger at

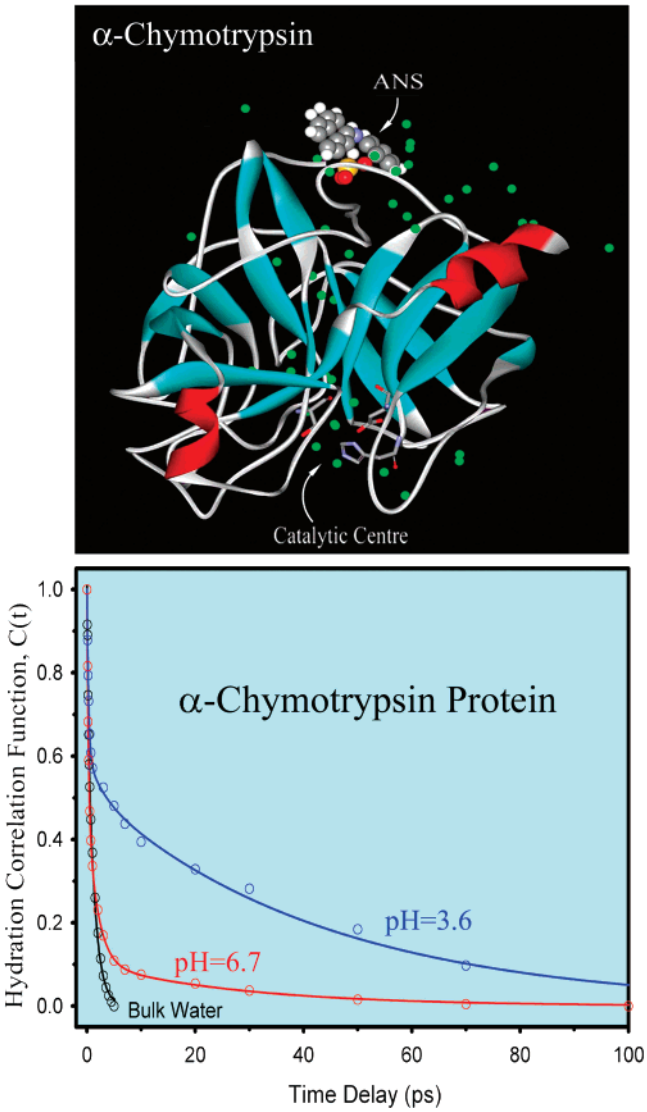

Figure 14. (Upper) X-ray structure of the protein α-chymotrypsin (CHT). The catalytic center in the hydrophobic pocket is indicated in the lower part of the structure. In the upper part, we show the probe ANS at its known binding site.[105] The structure was downloaded from the Protein Data Bank (2CHA) and handled with the program WEBLAB−VIEWERLITE. (Lower) Hydration correlation functions $C(t)$ of CHT−ANS in buffer solutions at pH 3.6 and 6.7. For comparison, we also include the $C(t)$ for ANS in bulk water.

higher pH, and, if anything, the contribution of free ANS to this component is smaller.

Given that the X-ray crystal structure is globally the same at different pHs, our observation that the hydration dynamics of ANS bound to CHT at pH 6.7 has a much larger contribution from the ultrafast, bulk-type hydration (90% of the spectral shift vs 50% at pH 3.6) indicates that, at this pH, the protein at the ANS-binding site exists in a state of hydration that is significantly different from that at lower pH; the site experiences much more of a bulk-type water at higher pH (Figure 14). Also, at the higher pH, the time constant of the slow component (28 ps) is shorter than that at pH 3.6 (43 ps), which again reflects a hydration from less rigid water layer than at lower pH. The ratio of amplitudes, bulk-type to rigid layer

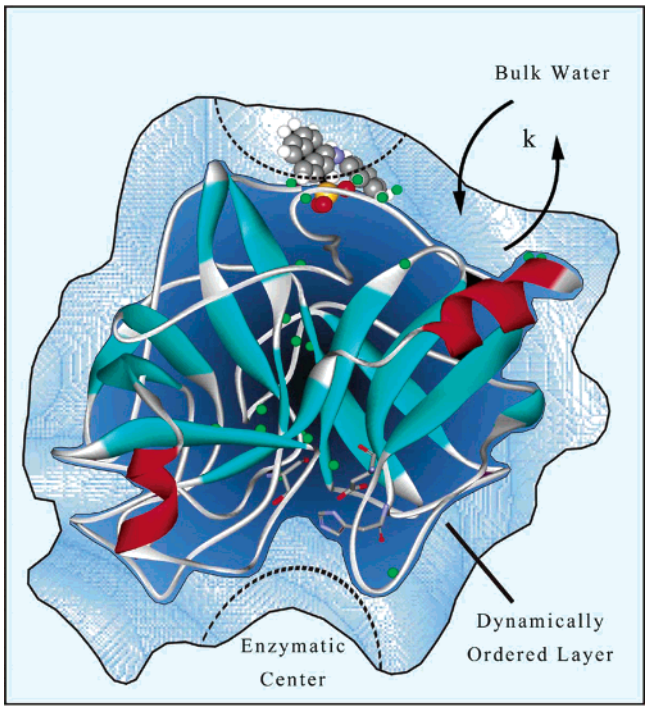

Figure 15. Simplified picture of the model emerging from the studies reported here. The dynamically ordered water is a general feature of the three proteins studied (see text). The function of the protein (α-chymotrypsin) at two pHs is illustrated by the degree of surface hydration and the rigidity of the water layer (see text).

behavior, has changed by at least an order of magnitude.

From our dynamical studies on the protein α-chymotrypsin, three significant points can be made. First, the longer hydration times at pH 3.6 and 6.7 (43 and 28 ps) are an order of magnitude slower than those of bulk water (∼1 ps), consistent with the general trend we observed for two other proteins, subtilisin *Carlsberg* and monellin.[7,9] Second, at pH 3.6, the contribution of the slower component in the hydration correlation function (43 ps) is much larger than that found for pH 6.7 (10%, 28 ps), reflecting a more structured water on the surface at low pH when the enzyme is inactive. Third, the drastic increase in the mobility of water, from the hydration correlation function, in the structured water layer is correlated with the function of the protein at high pH. Figure 15 presents a simplified picture of the role of hydration.

At low pH, the protonation of amino groups at the site studied presumably enhances positive charge interaction with the water layer.[104] Although the site of the protein we probed is not the reactive site, which is hydrophobic in nature[106] and near the enzymatic center, our findings may suggest a similar mechanism for the substrate−enzyme activity. The rigid water molecules at low pH (3.6) hinder the expression of protein functionality, while a mobile, less rigid water structure at high pH (6.7) makes the active recognition dynamically favorable—recognition and dehydration require rapid movement of water molecules.

More recently, we have studied the catalytic active site (hydrophobic pocket) by using two probes, one

covalently attached (anthraniloyl-chymotrypsin) and the other hydrophobically bonded (proflavine), and the biphasic behavior was recovered; time constants were ~1 (80%) and 23 ps (20%). An MD simulation[106] of the dynamics of water molecules in the pocket revealed that 10 of them stay inside the cavity at any given time, with large losses in hydrogen bonding among them. The loss of hydrogen bonding was attributed to the highly constrained geometry that prevents formation of an extended network, with only partial compensation by interactions with the protein. Thus, the solvent displacement concomitant with substrate binding would therefore be associated with a large enthalpic driving force. In this study, the average water−protein binding energy was found to be in the range of 2−3 kcal/mol. The effective residence time related to the binding energy is estimated to be in the range of 30−67 ps, taking the potential energy function for the transition from the bound to the free state to be a double Morse potential,[8] which is in the range of our measured value of 23 ps. However, from our study, the dynamics of water molecules in the active site is found to be nearly independent of the pH of the host buffer, revealing a specific role of these cavity water molecules in the chemistry of substrate hydrolysis rather than in the recognition processes, as mentioned above.[10]

In conclusion, these studies of the femtosecond dynamics of hydration of three proteins elucidate the nature of their surface interaction with water. However, the interaction with polar side chains (residues) of the protein near the surface must also be considered. In fact, for tryptophan in different proteins, the spectral shifts due to solvation by water and by side chains have been studied by MD simulations.[88] From an experimental point of view, surface hydration is evident for a number of reasons. First, from X-ray and NMR studies, the probe is at the surface for all three proteins, and the systematic spectroscopic shifts support the exposure to water; for example, in monellin and SC, the emission peaks are at 342 and 351 nm,[7,9] respectively, while for tryptophan inside a protein the peak is at 308 nm.[107] Recall that in bulk water tryptophan peaks at 356 nm, while in dioxane it peaks at 326 nm. The spectral shifts reflect the internal and *static* stark perturbation, which attractively or repulsively alters the energy levels at equilibrium, while *dynamical* solvation measures the fluctuations in energy as a function of time (see the theory section).

Second, the time-dependent anisotropy decays on a time scale that is much different from that of the hydration correlation function; in monellin, e.g., the anisotropy decays in 32 ps, followed by a longer time persistency, while the $C(t)$ longest decay is 16 ps and to the zero level; similar behavior was observed for SC, as discussed before. This suggests that the motion of an amino acid residue (anchored in the protein backbone) and its hydration occur on different time scales. Even if there are locally restricted fast motions of side chains, their collective solvation will require much longer time scales.

Third and finally, the fact that the $C(t)$ decay pattern and its two time scales are robust in three different proteins of different sequence and structure suggests the generality of their hydration picture, since the local side-chain structure in all three proteins is different and we expect a large change in the time scale for solvation. We know that, for bulk solvation of tryptophan, the effect of the environment (water, methanol, and ethanol) changes the decay of $C(t)$ by an order of magnitude. Even for DNA hydration, we recover the dynamics on the reported picosecond time scale for macromolecules, as discussed below.

5. DNA: Hydration and Function[11]

Water molecules at the surface of DNA are critical to the structure and to the recognition of other molecules, proteins, and drugs. The influence of drug binding on DNA hydration is striking. Acoustic and densimetric studies have shown[39,108] that a fraction (not all) of the water molecules is released upon recognition, hence the balance between enthalpic and entropic changes in determining the overall free energy of recognition. The degree of order in water dynamics is determined by the time scale of the motion and is important to the hydrophobic contribution. Recently, studies of solvation dynamics have been reported for an extrinsic chromogenic probe, inserted into DNA either by covalent adduction of coumarin dye[58] or by hydrophobic intercalation of acridine dye.[59] However, neither study gave the hydration dynamics in the DNA grooves (see the Introduction).

In principle, hydration dynamics can be investigated using the naturally occurring bases, but their fluorescence lifetimes are ultrashort[76,109,110] to give the full temporal evolution of water solvation. On the other hand, 2-aminopurine, a fluorescent analogue of the natural DNA base adenine, has a long lifetime and has been used to probe solvation dynamics of water and other polar solvents.[76] However, the efficient electron transfer between 2-aminopurine and the base guanine[111] does not allow for general interrogation of only water hydration.

In a recent paper, we presented our study of DNA hydration dynamics, with femtosecond resolution, in the minor groove (Figure 16), using the dodecamer B-DNA duplex d(CGCAAATTTGCG) whose X-ray structure without and with the drug Hoechst 33258 (H33258) has been reported;[112,113] the site for recognition is the minor groove and remains unchanged upon binding. We followed the time evolution of the Stokes shift of the fluorescence of the drug, bound to DNA, and obtained the decay of the hydration correlation function. The function reflects the rotational and translational motions of water molecules in the minor groove. We also reported our study of calf thymus DNA upon binding to the same drug (H33258) in order to compare with the dodecamer DNA. Finally, to probe the rigidity of the drug and the time scale of its motion with DNA, we examined the time-resolved polarization anisotropy, $r(t)$.

The $C(t)$ function, as shown in Figure 17, is biphasic, a sum of two exponentials with the time

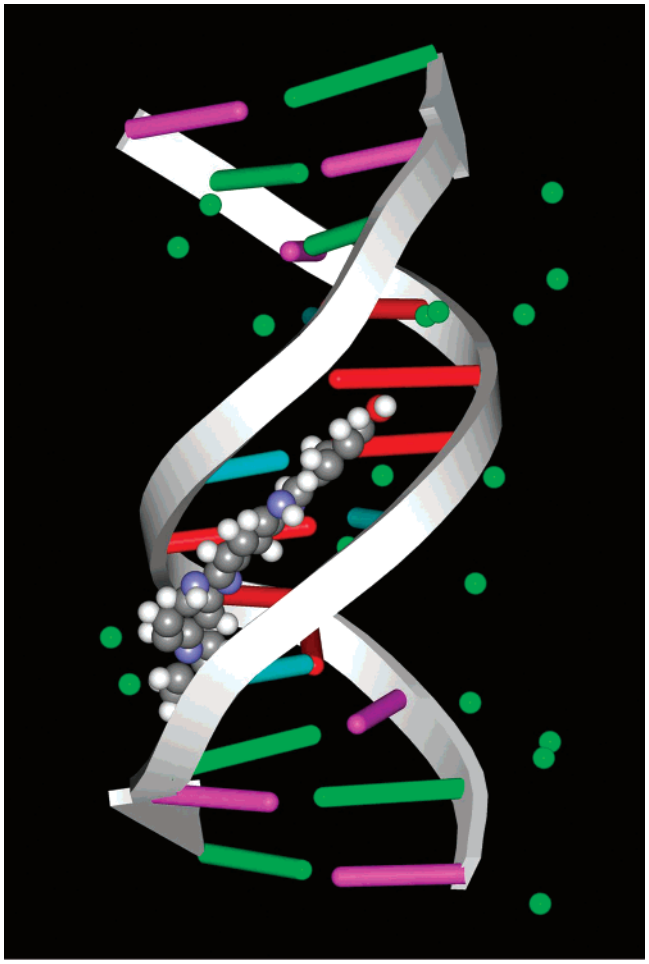

Figure 16. X-ray structure of the drug Hoechst 33258 with the dodecamer duplex DNA. The structure was downloaded from the Protein Data Bank (264D) and handled with the program WEBLAB−VIEWERLITE. In the absence of the drug there are 71 water molecules with the dodecamer,[112] and in the presence of the drug only 18 water molecules (green balls) are present.

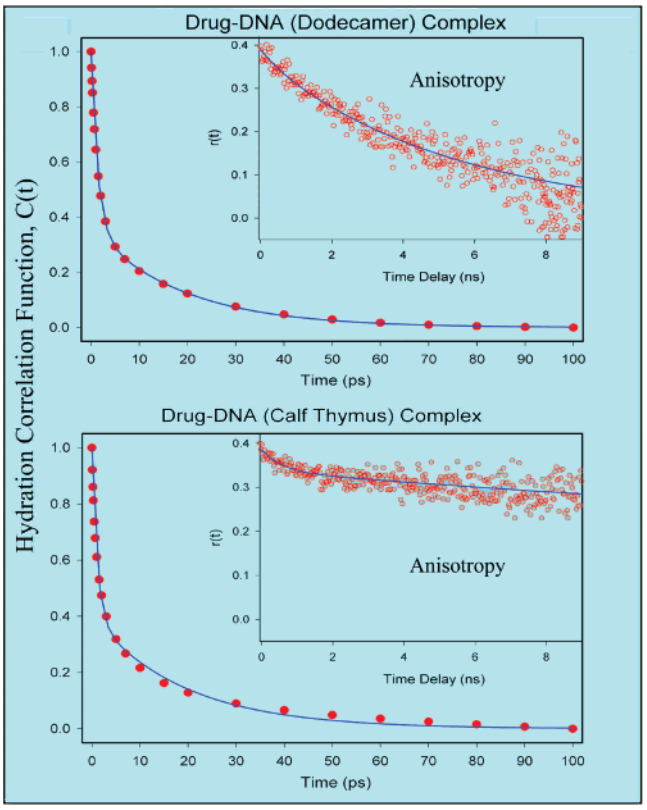

Figure 17. (Upper) Hydration correlation function $C(t)$ of the DNA−drug complex obtained from femtosecond-resolved experiments. Inset: The time-resolved anisotropy $r(t)$ of the probe drug in the complex at emission wavelength 510 nm, with excitation at 400 nm (using single photon counting). (Lower) Hydration correlation function $C(t)$ of the complex. (Lower) The time-resolved anisotropy $r(t)$ of the probe drug in the complex at emission wavelength 510 nm, with excitation at 400 nm (using single photon counting). Note the difference in time scales between $C(t)$ and $r(t)$, and between the anisotropies of duplex and calf thymus DNA.

constants of 1.4 (64%) and 19 ps (36%); any sub-100 fs components in these dynamics are unresolved. The net spectral shift observed is 1304 cm^{-1}. To ascertain the degree of orientational rigidity of the drug in the complex, we obtained the $r(t)$ decay at 510 nm using single photon counting. The $r(t)$ is observed (Figure 17, inset) to decay with time constants of 600 ps (5%) and 5.5 ns (95%) (the estimated hydrodynamic rotational relaxation times of the complex are 50 and 10 ns for the stick and slip limit, respectively). The one order of magnitude lengthening of the drug anisotropy decay in the dodecamer, compared to that in the bulk, is consistent with a rigid drug binding in the minor groove; the whole complex changes its orientation on the nanosecond time scale.

The $C(t)$ function for the calf thymus DNA in Figure 17 is also biexponential (time constants of 1.1 (60%) and 19 ps (40%)). The net spectral shift observed is 1582 cm^{-1}. The time constants along with their contributions are similar to those observed in the dodecamer duplex. But, the fluorescence anisotropy at 510 nm decays with different time constants: 600 ps (12%) and 55 ns (88%), compared to 600 ps (5%) and 5.5 ns (95%) in the duplex. Again, this is consistent with the fact that natural calf thymus DNA is much longer than duplex DNA (12 pairs of bases only).

The observed bimodality (Figures 17 and 18) in surface hydration of DNA(s) is in fact consistent with our previous reports[7,9,10] on hydration dynamics at protein surfaces. The DNA hydration time of 19 ps (40%) for the weakly bound water is in line with those observed for the protein surface hydration: subtilisin *Carlsberg* (38 ps, 39%), monellin (16 ps, 54%), and α-chymotrypsin (28 ps, 10%). Relating these times of the correlation functions to residence times in the water layer identifies the effect of first shell polarization due to the restricted motions of water molecules by rotational and translational diffusion, as discussed in the theory section. These residence times are for the weakest-bound, water since our measurements span the earliest possible (femtosecond) time scale.

Considering the equilibrium between water molecules and the DNA sites, a residence time of minor grooves with $k_{off} \approx 5 \times 10^{10}$ s^{-1} and a diffusion-controlled k_{on} of $\sim 10^{10}$ M^{-1} s^{-1} [114] gives $K_d \approx 5$ M, so that each accessible site on the average would be in contact with water for more than 90% of the time—the site has very high occupancy at equilibrium. Dynamically speaking, however, the site is in ex-

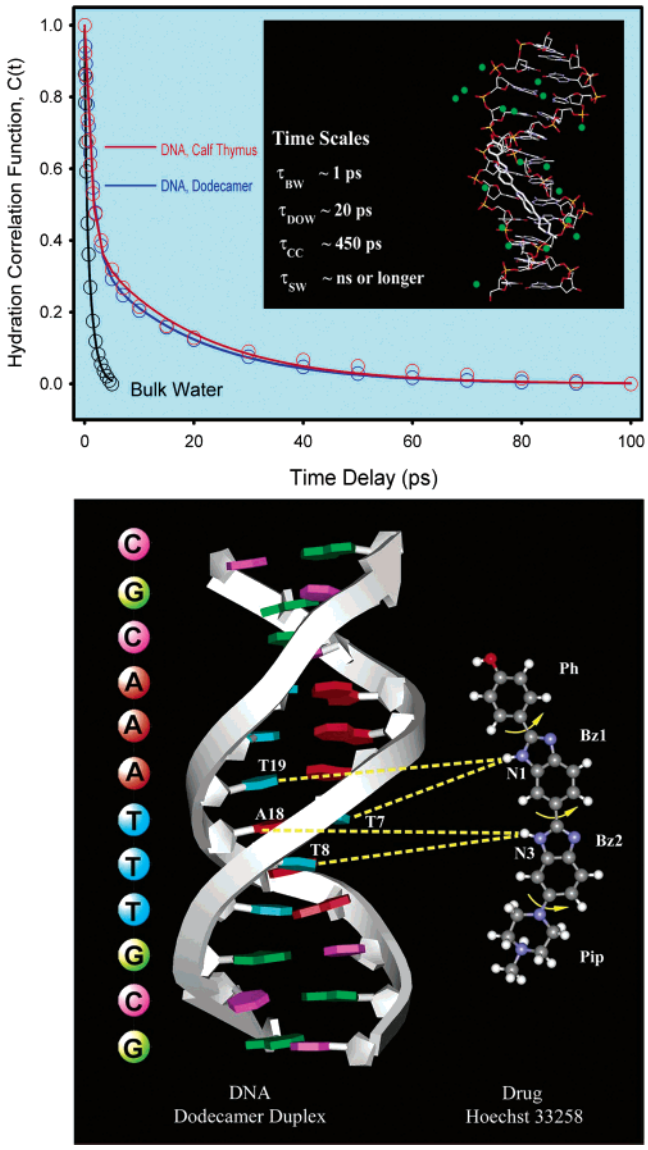

Figure 18. (Upper) Comparison of the hydration correlation functions for the drug−DNA (dodecamer and calf thymus) complexes in aqueous buffer solutions. We also include the result for the drug in bulk water (buffer) for comparison. Inset: The structured water (green balls) with the drug in the minor groove (see text), according to X-ray studies.[113] The time scales given denote τ_{BW} (bulk water), τ_{DOW} (dynamically ordered water), τ_{CC} (conformational change water), and τ_{SW} (structural water); see text. (Lower) Molecular structures of the drug Hoechst 33258 and its interaction with the dodecamer DNA, with the sequence indicated. The four moieties of the drug structure are depicted: a piperazine (nonaromatic) ring (Pip), two benzimidazole (aromatic) rings (Bz1 and Bz2), and a phenyl (aromatic) ring (Ph). Possible free rotations about the connecting bonds are indicated with arrows. Two three-centered hydrogen bonds between the drug (two N−H bonds of N1 and N3) and DNA bases are shown, based on the crystal structure.[113] At neutral pH, the drug molecule (trihydrochloride form) has only one positive charge on the terminal nitrogen atom of the Pip ring.[143] In the view presented, the drug is projected out from the minor groove (see Figure 16); the atom colors for the drug are red for oxygen, white for hydrogen, blue for nitrogen, and gray for carbon.

change with the bulk, destroying the order on the picosecond time scale, and this is the origin of the bimodality, as discussed above.

The residence time for ordered water relative to other time constants of DNA critically determines the stability and recognition. First, we must consider the time scale of making and breaking bonds of the dynamically ordered water, τ_{DOW}, relative to that of structural conformational changes, τ_{CC}, by bending and twisting,[115] which involve the structurally ordered water. The value of τ_{CC} is important to, e.g., the change of the B form of DNA to A and Z forms whose relative stabilities depend on the water content and sequence; the B form predominates in aqueous solution. If τ_{DOW} is shorter than τ_{CC}, then recognition is an effective process with structural integrity. The loss of order on the picosecond time scale is significant in changing the entropy, and it is possible that this contribution to the free energy is governed by the change in the rotations of water molecules.

Second, it is important to compare the residence time of weakly bound water, τ_{DOW}, with the time of breaking/making hydrogen bonds, τ_{HB}, in bulk water. With a barrier of a few kilocalories per mole, kinetically τ_{HB} is on the order of a few picoseconds, and for an effective recognition, τ_{DOW} should not be orders of magnitude longer than the value of τ_{HB}, so that the efficiency becomes optimum. If $\tau_{DOW}/\tau_{HB} \approx 1$, then the degree of order is that of the bulk.

Last, we consider the time scale for the motion of the drug in the groove, by orientational diffusion, τ_{OD}, relative to τ_{DOW}. For the drug studied here, τ_{OD} is much longer than τ_{DOW} for both types of DNA, as evidenced by the anisotropy, ensuring a well-defined geometry, certainly on the time scale of dynamically ordered water.

The robustness of the range of values for the hydration times in DNA (and proteins) is indicative of the nature of the layer, being ordered on the molecular scale even in the presence of the drug. This picture is consistent with the results of an NMR study[114] on the hydration and solution structure of the duplex sequence we have used and its complex with a minor-groove-binding drug, propamidine. It was found that complexation with the drug has *little effect* on the residence times for water molecules bound either in the major groove or at the sites in the minor groove. The range of residence times was found to be ~0.2−0.4 ns for surface water at the grooves; the residence times of water molecules in the major groove are only an order of magnitude shorter than those for the most long-lived waters in the minor groove.

From the above discussion, two points should be emphasized. Our above-mentioned results of hydration dynamics in the two DNA systems studied were obtained by using the time window from 0 up to 200 ps. Longer-time Stokes shifts may be present, reflecting the influence of more rigid water structure on the time scale indicated by NMR studies.[33,116] However, the resemblance of the evolving spectra to the maximum of the steady-state fluorescence spectrum[11] in 100 ps ($\nu_{max}(\infty)$) indicates that most of the dynamics are complete within our time window, but a fraction of strongly bound water may still be present with a time scale of sub-nanoseconds or longer (we

measured the lifetime of the drug in the dodecamer and found it to be 1.8 and 4.3 ns, consistent with the values in the literature[84]). Clearly, because of our time window, the experiments probe the dynamically ordered water, the weakest in binding, which is critical to the function. Much longer residence times may reflect water of structural purpose.

Because the ordered water is probed here around the drug in the grooves, one must not ignore such water in the recognition process and in drug design strategies.[117] In fact, studies using densimetric and ultrasonic measurements have shown that a minor-groove-binding drug, netropsin, displaces, depending on the base sequence, a significant number of water molecules upon complexation with a DNA duplex.[39] We note that thermodynamic measurement of the release of water is concerned with essentially all waters occupied in the grooves, while the dynamics experiments can detect only a small subpopulation of a certain net of interfacial water molecules that contribute to ligand binding. The dynamics of the ordered water and its loss by, e.g., rotational diffusion must contribute to the entropic process involved.

From a structural point of view, the drug studied here (Figure 18) binds in the minor groove, covering the sequence AATTT of the central A-tract, with the piperazine group close to one of the GC regions. It makes two three-centered hydrogen bonds from the nitrogen atoms of benzimidazole rings to the N (A18) and O (T7, T8, T19) atoms of the DNA bases. This hydrogen bonding (and electrostatic/dispersion interactions) is facilitated by the presence of ordered water (entropic) around the drug; if ordered water is involved in direct binding of the drug, then enthalpic contributions must also be included. Hydrogen bonding is also possible for the drug (Figure 18; nitrogens opposite to N1 and N3) with water near the surface of the groove, which is more of a bulk type in our bimodal distribution of hydration. The most weakly bound water molecules are of critical importance to biological function[118] and are unlikely to be seen in crystal structures or by NMR.[118] They are part of the total hydration which influences the structural and biological activities.[119,120] The residence times of weakly bound water are only an order of magnitude different from that of the bulk, and they are the ones that have to be probed with femtosecond resolution.

In conclusion, these first studies to characterize, with femtosecond resolution, the time scale of hydration/dehydration at the DNA surface are particularly revealing of the nature of water dynamics in a known local structure and with a drug in the minor groove. The fact that the water is dynamically ordered at the surface of DNA without spatial averaging or position inhomogeneity of the drug allows us to observe the earliest processes of hydration dynamics. Recognition of minor grooves by charge and shape complementarities, and using directional hydrogen bonds, cannot be fully understood from a static structure without including the role of water and the time scale for the loss of the order. It may turn out that this dynamically ordered water is also crucial for interfacial recognition, not only of drugs but also between macromolecules.

6. Conclusion

In this review, we have addressed some key issues of biomolecular hydration, with emphasis on proteins in the native (and denatured) state and on DNA of two types, synthetic dodecamer duplex and genomic calf thymus. The femtosecond time resolution provides us with the opportunity of mapping out hydration dynamics on the time scale of the actual molecular motions of water and at the earliest times. On this time scale, it is possible to examine the dynamical nature of water in the bulk and the water loosely bound in the interfacial layer.

The use of the intrinsic amino acid (tryptophan) as a single site probe on the surface of the protein native structure, known from X-ray and NMR studies, and the use of probes covalently attached to the protein, or drugs in the minor groove of DNA, allow us to follow the change in hydration as a function of time (femtosecond and picosecond) and to estimate the layer thickness ($\leq$7 Å) without disturbance of the native structure. Through this change in the spectral properties of the probe molecule—at early times, the spectrum is that of a nonequilibrated structure ("blue spectra"), and at longer times it reaches the equilibrium state ("red spectra")—we construct the hydration correlation function, which represents the solvent energy fluctuation, and obtain the fundamental time constants for solvation. For comparison, we also studied the same probe in bulk water.

The results for biomolecular hydration are vastly different from those of bulk water and identify two types (biphasic) of water at the interface: those which are labile, or bulklike ($\sim$1 ps), and those which are bound to the surface ($\sim$20−40 ps). The equilibrium between the two types of water in the layer and the "feedback" of water from the bulk (by translational and rotational diffusions) have been formulated in a simple theoretical model which reproduces the experimental results. The contribution to solvation by the side chains (residues) of the macromolecules was considered, but the experimental evidence against it comes from the following: X-ray and NMR studies which identify the probe at the surface, and the *systematic* spectral shifts with time which are also consistent with surface location; the robustness of the observed biphasic behavior of hydration and the time scales, despite changes in the sequence and structure of the macromolecule (the robustness of hydration behavior has recently been found in theoretical MD simulations of isothermal compressibilities of hydrated proteins[121]); and the significant difference between the decays of the anisotropy and those of hydration correlation functions. In all studies we measured the time-dependent anisotropy of emission in order to determine the rigidity of the probe molecule and to ascertain the flexibility of a residue like tryptophan.

Besides the femtosecond temporal resolution, these experiments of hydration provide a unique spatial resolution. The spatial resolution in this case is determined by the (single) molecular probe used at the surface of the protein (or in the minor groove of DNA) and its interaction with the surrounding water in a region determined by the R^{-3} dependence of the

interaction between the probe dipole and water molecules. Hydration of biomolecules through weak forces is a dynamical process which defines a molecular layer on the scale of a few angstroms. The picosecond time scale of the dynamics excludes a static iceberg-type model, and it is clear that such ultrafast mobility, by rotational and translational motions, are unique in determining the hydrogen-bonded layer ordering, and hence the structure and function.

For the structure, the hydrophobic collapse in the interior of the protein and the hydrophilic interaction with hydrogen-bonded water results in entropic and enthalpic changes which are determinants of the net free energy of stability. For the function, water in the layer has a finite residence time and its dynamics is an integral part of processes of two general categories—molecular recognition and reactions at the active site. Examples include selective molecular recognition of ligands (substrate) through the unique directionality and adaptability of the hydrogen bond and water motion; enzymatic activity mediated by water located at the molecular distance scale, not diffusive; and protein−protein association[122] through water mediation by entropic water displacement (desolvation) and energetic minimization of charge repulsion.

With this in mind, the time scale for the dynamics is uniquely positioned—it must be longer than the bulk dynamics and shorter than the time for the unfolding of the active structure. To maintain selectivity and order in the layer, the picosecond time scale seems ideal. For example, for DNA recognition of the drug studied here, the time scale of the twisting and bending of DNA[115] and that of hydration determine the efficacy of recognition for an "intact" double-strand structure in bulk water. Diffusion of the binding ligand is slow, but at the interface the motion of the water molecules is ultrafast in order to optimize entropic and enthalpic interactions.

The new generations of experiments should link these dynamical studies of these and other processes to the function. We have already begun research in this direction. In a recent publication,[123] we reported studies of the femtosecond dynamics of an RNA−protein (peptides) complex and then compared the results with those obtained for in vivo (*Escherichia coli*) transcription anti-termination activities. In another study,[124] we measured the activity of the enzyme subtilisin *Carlsberg*, discussed above, with substrates Ala-Ala-Phe-7-amido-4-methylcoumarin and succinyl-Ala-Ala-Pro-Phe-*p*-nitroanilide. From Michaelis−Menten kinetics we obtained the catalytic rates, and using the surface probe (native) tryptophan of the protein we obtained the femtosecond and picosecond hydration dynamics in different solvents (dioxane, acetonitrile, and aqueous solutions). In this way, we examined the influence of solvation on reactivity in aqueous and nonaqueous environments, since the structures were found to be in the native state for all these solvents;[125] such studies explore the possible "poisoning" caused by agents (used, e.g., in food processing) other than water. Currently, we are completing studies of ligand recognition by myoglobin and hemoglobin on the femtosecond and longer time scales to compare with model systems we studied earlier using picket-fence porphyrin and molecular oxygen.[126]

In this review, we have not discussed other publications from Caltech in this general area of biological studies. It may be helpful to list the relevant references for these studies: DNA electron transfer[111,127−129] and DNA−anticancer (daunomycin) drug;[130] human serum albumin ligand recognition;[131] dioxygen picket-fence porphyrins;[126,132] protein−DNA recognition complex;[72] riboflavin binding protein and glucose oxidase enzyme;[133] drug (daunomycin)−protein complexes;[134] energy transfer and solvation in protein rubredoxin;[66] proton transfer in model base pairs;[135−137] nonradiative processes of DNA/RNA nucleotides and nucluosides;[76,109] and studies of free base tetraphenylporphyrin[138] and zinc tetraphenylporphyrin.[139] More recent publications, added in proofs, have centered on studies of site- and sequence-selective DNA hydration,[140] ordered water at the interface of enzyme−substrate (micelle) complex,[141] and temperature gating of electron transfer in DNA.[142] The goal in all these studies is to relate structures to the dynamics and, it is hoped, to key features of the (complex!) function.

7. Acknowledgment

This work was supported by the National Science Foundation. We thank colleagues in our laboratory at Caltech whose contributions over the years, acknowledged in the references, have been instrumental in the successful evolution of work in this area. In particular, for the studies of hydration of macromolecules, we thank Drs. Dongping Zhong, Jorge Peon, Liang Zhao, Sarika M. Bhattacharyya, Amisha Kamal, and Professor Biman Bagchi, who was a visiting associate at Caltech (spring 2002). We acknowledge the valuable discussions with Drs. Tianbing Xia and Spencer Baskin.

8. References

(1) Rupley, J. A.; Cateri, G. *Adv. Protein Chem.* **1991**, *41*, 37.
(2) Kornblatt, J. A.; Kornblatt, M. J. *Int. Rev. Cytol.* **2002**, *215*, 49.
(3) Pocker, Y. *Cell. Mol. Life Sci.* **2000**, *57*, 1008.
(4) Gregory, R. B. *Protein Solvent Interactions*; Dekker: New York, 1995.
(5) Finney, J. L. *Faraday Discuss.* **1996**, *103*, 1 (see references therein, and the entire issue).
(6) Harding, S. E. *Biophys. Chem.* **2001**, *93*, 87 (see the entire issue).
(7) Pal, S. K.; Peon, J.; Zewail, A. H. *Proc. Natl. Acad. Sci. U.S.A.* **2002**, *99*, 1763.
(8) Pal, S. K.; Peon, J.; Bagchi, B.; Zewail, A. H. *J. Phys. Chem. B* **2002**, *106*, 12376 and references therein.
(9) Peon, J.; Pal, S. K.; Zewail, A. H. *Proc. Natl. Acad. Sci. U.S.A.* **2002**, *99*, 10964.
(10) Pal, S. K.; Peon, J.; Zewail, A. H. *Proc. Natl. Acad. Sci. U.S.A.* **2002**, *99*, 15297.
(11) Pal, S. K.; Zhao, L.; Zewail, A. H. *Proc. Natl. Acad. Sci. U.S.A.* **2003**, *100*, 8113.
(12) Bernal, J. D.; Crowfoot, D. *Nature (London)* **1934**, *133*, 794.
(13) Adair, G. S.; Adair, M. E. *Proc. R. Soc. B* **1936**, *120*, 422.
(14) Retgers, J. W. *Z. Phys. Chem.* **1889**, *3*, 289.
(15) Svedberg, T. *Kolloid Z.* **1930**, *51*, 10.
(16) Sorensen, S. L. P. *C. R. Lab. Carlsberg* **1917**, *12*.
(17) Perutz, M. F. *Biosystems* **1977**, *8*, 261.
(18) Takano, T. *J. Mol. Biol.* **1977**, *110*, 533.
(19) Kauzmann, W. *Adv. Protein Chem.* **1959**, *14*, 1.

(20) Makarov, V.; Pettitt, B. M.; Feig, M. *Acc. Chem. Res.* **2002**, *35*, 376.
(21) Bizzarri, A. R.; Cannistraro, S. *J. Phys. Chem. B* **2002**, *106*, 6617.
(22) Nandi, N.; Bhattacharyya, K.; Bagchi, B. *Chem. Rev.* **2000**, *100*, 2013.
(23) Eisenthal, K. B. *Acc. Chem. Res.* **1993**, *26*, 636.
(24) Ball, P. *Nature (London)* **2003**, *423*, 25.
(25) Chandler, D. *Nature (London)* **2002**, *417*, 491.
(26) Michael, D.; Benjamin, I. *J. Chem. Phys.* **2001**, *114*, 2817.
(27) Southhall, N. T.; Dill, K. A.; Haymet, A. D. J. *J. Phys. Chem. B* **2002**, *106*, 521.
(28) Whitesides, G. M.; Grzybowski, B. *Science* **2002**, *295*, 2418.
(29) Cheng, X.; Schoenborn, B. P. *J. Mol. Biol.* **1991**, *220*, 381.
(30) Gu, W.; Schoenborn, B. P. *Proteins: Struct., Funct. Genet.* **1995**, *22*, 20.
(31) Nandi, N.; Bagchi, B. *J. Phys. Chem. B* **1997**, *101*, 10954.
(32) Roccchi, C.; Bizzarri, A. R.; Cannistraro, S. *Phys. Rev. E: Stat. Phys., Plasmas, Fluids, Relat. Interdiscip. Top.* **1998**, *57*, 3315.
(33) Halle, B.; Denisov, V. P. *Biopolymers* **1998**, *48*, 210.
(34) Otting, G.; Liepinsh, E.; Wuthrich, K. *Science* **1991**, *254*, 974.
(35) Wüthrich, K.; Billeter, M.; Güntert, P.; Luginbühl, P.; Riek, R.; Wider, G. *Faraday Discuss.* **1996**, *103*, 245.
(36) Denisov, V. P.; Halle, B. *Faraday Discuss.* **1996**, *103*, 227.
(37) Dervan, P. B. *Bioorg. Med. Chem.* **2001**, *9*, 2215 and references therein.
(38) Schneider, B.; Cohen, D.; Berman, H. M. *Biopolymers* **1992**, *32*, 725.
(39) Chalikian, T. V.; Plum, G. E.; Sarvazyan, A. P.; Breslauer, K. J. *Biochemistry* **1994**, *33*, 8629.
(40) Umehara, T.; Kuwabara, S.; Mashimo, S.; Yagihara, S. *Biopolymers* **1990**, *30*, 649.
(41) Feig, M.; Pettitt, B. M. *Biopolymers* **1998**, *48*, 199.
(42) Duan, Y.; Wilkosz, P.; Crowley, M.; Rosenberg, J. M. *J. Mol. Biol.* **1997**, *272*, 553.
(43) Drew, H. R.; Dickerson, R. E. *J. Mol. Biol.* **1981**, *151*, 535.
(44) Leipinsh, E.; Otting, G.; Wuthrich, K. *Nucleic Acids Res.* **1992**, *20*, 6549.
(45) Chuprina, V. P. *Nucleic Acids Res.* **1987**, *15*, 293.
(46) Bagchi, B. *Annu. Rev. Phys. Chem.* **1989**, *40*, 115.
(47) Fleming, G. R.; Cho, M. *Annu. Rev. Phys. Chem.* **1996**, *47*, 109.
(48) Bagchi, B.; Biswas, R. *Adv. Chem. Phys.* **1999**, *109*, 207.
(49) Jimenez, R.; Fleming, G. R.; Kumar, P. V.; Maroncelli, M. *Nature* **1994**, *369*, 471.
(50) Hynes, J. T. *J. Phys. Chem.* **1986**, *90*, 3701.
(51) Jarzeba, W.; Walker, G.; Johnson, A. E.; Kahlow, M. A.; Barbara, P. F. *J. Phys. Chem.* **1988**, *92*, 7039.
(52) Maroncelli, M.; Fleming, G. R. *J. Chem. Phys.* **1987**, *86*, 6221.
(53) Onsager, L. *Can. J. Chem.* **1977**, *55*, 1819.
(54) Stratt, R. M.; Maroncelli, M. *J. Phys. Chem.* **1996**, *100*, 12981.
(55) Hsu, C.-P.; Song, X.; Marcus, R. A. *J. Phys. Chem. B* **1997**, *101*, 2546.
(56) Changenet-Barret, P.; Choma, C. T.; Gooding, E. F.; DeGrado, W. F.; Hochstrasser, R. M. *J. Phys. Chem. B* **2000**, *104*, 9322.
(57) Jordanides, X. J.; Lang, M. J.; Song, X.; Fleming, G. R. *J. Phys. Chem. B* **1999**, *103*, 7995.
(58) Brauns, E. B.; Madaras, M. L.; Coleman, R. S.; Murphy, C. J.; Berg, M. A. *J. Am. Chem. Soc.* **1999**, *121*, 11644.
(59) Hess, S.; Davis, W. B.; Voityuk, A. A.; Rosch, N.; Michel-Beyerle, M. E.; Ernsting, N. P.; Kovalenko, S. A.; Lustres, J. L. P. *ChemPhysChem* **2002**, *3*, 452.
(60) Bhattacharyya, S. M.; Wang, Z.-G.; Zewail, A. H. *J. Phys. Chem. B* **2003**, *107*, 13218.
(61) Nienhuys, H. K.; Santen, R. A. V.; Bakker, H. J. *J. Chem. Phys.* **2000**, *112*, 8487.
(62) Price, W. S.; Ide, H.; Arata, Y. *J. Phys. Chem. A* **1999**, *103*, 448.
(63) Horng, M. L.; Gardecki, J. A.; Papazyan, A.; Maroncelli, M. *J. Phys. Chem.* **1995**, *99*, 17311.
(64) Suppan, P.; Ghoneim, N. *Solvatochromism*; The Royal Society of Chemistry: Cambridge UK, 1997.
(65) Caldin, E. F. *The Mechanisms of Fast Reactions in Solution*; IOS Press: Oxford, 2001.
(66) Zhong, D.; Pal, S. K.; Zhang, D.; Chan, S. I.; Zewail, A. H. *Proc. Natl. Acad. Sci. U.S.A.* **2002**, *99*, 13.
(67) McMahon, L. P.; Yu, H. T.; Vela, M. A.; Morales, G. A.; Shui, L.; Fronczek, F. R.; McLaughlin, M. L.; Barkley, M. D. *J. Phys. Chem. B* **1997**, *101*, 3269.
(68) Szabo, A. G.; Rayner, D. M. *J. Am. Chem. Soc.* **1980**, *102*, 554.
(69) Shen, X. H.; Knutson, J. *J. Phys. Chem. B* **2001**, *105*, 6260.
(70) Callis, P. R. *J. Chem. Phys.* **1991**, *95*, 4230.
(71) Ruggiero, A. J.; Todd, D. C.; Fleming, G. R. *J. Am. Chem. Soc.* **1990**, *112*, 1003.
(72) Zhong, D.; Pal, S. K.; Zewail, A. H. *ChemPhysChem* **2001**, *2*, 219.
(73) DeToma, R. P.; Easter, J. H.; Brand, L. *J. Am. Chem. Soc.* **1976**, *98*, 5001.
(74) Zhang, J.; Bright, F. V. *J. Phys. Chem.* **1991**, *95*, 7900.
(75) Kosower, E. M. *Acc. Chem. Res.* **1982**, *15*, 259.
(76) Pal, S. K.; Peon, J.; Zewail, A. H. *Chem. Phys. Lett.* **2002**, *363*, 57 and references therein.
(77) Nordlund, T. M.; Andersson, S.; Nilsson, L.; Rigler, R.; Gräslund, A.; McLaughlin, L. W. *Biochemistry* **1989**, *28*, 9095.
(78) Sowers, L. C.; Fazakerley, G. V.; Eritja, R.; Kaplan, B. E.; Goodman, M. F. *Proc. Natl. Acad. Sci. U.S.A.* **1986**, *83*, 5434.
(79) Holmén, A.; Nordén, B.; Albinsson, B. *J. Am. Chem. Soc.* **1997**, *119*, 3114.
(80) Rachofsky, E. L.; Ross, J. B. A.; Krauss, M.; Osman, R. *Acta Phys. Pol. A* **1998**, *94*, 735.
(81) Denham, D. A.; Suswillo, R. R.; Rogers, R.; McGreevy, P. B.; Andrew, B. J. *J. Helminthol.* **1976**, *50*, 243.
(82) Latt, S. A.; Stetten, G. *J. Histochem. Cytochem.* **1976**, *24*, 24.
(83) Gorner, H. *Photochem. Photobiol.* **2001**, *73*, 339.
(84) Cosa, G.; Focsaneanu, K.-S.; McLean, J. R. N.; McNamee, J. P.; Scaiano, J. C. *Photochem. Photobiol.* **2001**, *73*, 585.
(85) Kalninsh, K. K.; Pestov, D. V. *J. Photochem. Photobiol. A: Chem.* **1994**, *83*, 39.
(86) Chapman, C. F.; Fee, R. S.; Maroncelli, M. *J. Phys. Chem.* **1995**, *99*, 4811.
(87) Elsaesser, T.; Kaiser, W. *Annu. Rev. Phys. Chem.* **1991**, *42*, 83.
(88) Vivian, J. T.; Callis, P. R. *Biophys. J.* **2001**, *80*, 2093.
(89) Haugland, R. P. *Handbook of Fluorescent Probes and Research Chemicals*, 6th ed.; Molecular Probes: Eugene, OR, 1996; pp 8−13.
(90) Ren, B.; Gao, F.; Tong, Z.; Yan, Y. *Chem. Phys. Lett.* **1999**, *307*, 55.
(91) Voet, D.; Voet, J. G. *Biochemistry*, 2nd ed.; Wiley: Somerset, NJ, 1995; pp 398−400.
(92) Morris, J. A.; Cagan, R. H. *Biochim. Biophys. Acta* **1972**, *261*, 114.
(93) Morris, J. A.; Martenson, R.; Deibler, G.; Cagan, R. H. *J. Biol. Chem.* **1973**, *248*, 534.
(94) Cagan, R. H. *Science* **1973**, *181*, 32.
(95) Somoza, J. R.; Cho, J. M.; Kim, S.-H. *Chem. Senses* **1995**, *20*, 61.
(96) Ogata, C.; Hatada, M.; Tomlinson, G.; Shin, W. C.; Kim, S. H. *Nature (London)* **1987**, *328*, 739.
(97) Somoza, J. R.; Jiang, F.; Tong, L.; Kang, C. H.; Cho, J. M.; Kim, S. H. *J. Mol. Biol.* **1993**, *234*, 390.
(98) Lee, S.-Y.; Lee, J.-H.; Chang, H.-J.; Cho, J. M.; Jung, J.-W.; Lee, W. *Biochemistry* **1999**, *38*, 2340.
(99) Swaminathan, R.; Krishnamoorthy, G.; Periasamy, N. *Biophys. J.* **1994**, *67*, 2013.
(100) Robertson, W. H.; Diken, E. G.; Johnson, M. A. *Science* **2003**, *301*, 320.
(101) Omta, A. W.; Kropman, M. F.; Woutersen, S.; Bakker, H. J. *Science* **2003**, *301*, 347.
(102) Zubay, G. *Biochemistry*; Addison-Wesley: Reading, MA, 1983; Chapter 4, pp 130−175.
(103) Charman, W. N.; Porter, C. J. H.; Mithani, S.; Dressman, J. B. *J. Pharm. Sci.* **1997**, *86*, 269.
(104) Johnson, J. D.; El-Bayoumi, M. A.; Weber, L. D.; Tulinsky, A. *Biochemistry* **1979**, *18*, 1292.
(105) Weber, L. D.; Tulinsky, A.; Johnson, J. D.; El-Bayoumi, M. A. *Biochemistry* **1979**, *18*, 1297.
(106) Carey, C.; Cheng, Y.-K.; Rossky, P. J. *Chem. Phys.* **2000**, *258*, 415.
(107) Lakowicz, J. R. *Principles of fluorescence spectroscopy*; Kluwer Academic/Plenum: New York, 1999; Chapter 16, pp 445−486.
(108) Chalikian, T. V.; Volker, J.; Srinivasan, A. R.; Olson, W. K.; Breslauer, K. J. *Biopolymers* **1999**, *50*, 459.
(109) Peon, J.; Zewail, A. H. *Chem. Phys. Lett.* **2001**, *348*, 255.
(110) Gustavsson, T.; Sharonov, A.; Onidas, D.; Markovitsi, D. *Chem. Phys. Lett.* **2002**, *356*, 49.
(111) Wan, C.; Fiebig, T.; Schiemann, O.; Barton, J. K.; Zewail, A. H. *Proc. Natl. Acad. Sci. U.S.A.* **2000**, *97*, 14052.
(112) Edwards, K. J.; Brown, D. G.; Spink, N.; Skelly, J. V.; Neidle, S. *J. Mol. Biol.* **1992**, *226*, 1161.
(113) Vega, M. C.; Saez, I. G.; Aymami, J.; Eritja, R.; Marel, G. A. V. D.; Boom, J. H. V.; Rich, A.; Coll, M. *Eur. J. Biochem.* **1994**, *222*, 721.
(114) Lane, A. N.; Jenkins, T. C.; Frenkiel, T. A. *Biochim. Biophys. Acta* **1997**, *1350*, 205.
(115) Millar, D. P.; Robbins, R. J.; Zewail, A. H. *J. Chem. Phys.* **1982**, *76*, 2080 and references therein.
(116) Denisov, V. P.; Carlstrom, G.; Venu, K.; Halle, B. *J. Mol. Biol.* **1997**, *268*, 118.
(117) Haq, I. *Arch. Biochem. Biophys.* **2002**, *403*, 1.
(118) Rand, R. P. *Science* **1992**, *256*, 618.
(119) Mrevlishvili, G. M.; Carvalho, A. P. S. M. C.; da Silva, M. A. V. R.; Mdzinarashvili, T. D.; Razmadze, G. Z.; Tarielashvili, T. Z. *J. Therm. Anal. Cal.* **2001**, *66*, 133.
(120) Robinson, C. R.; Sligar, G. *J. Mol. Biol.* **1993**, *234*, 302.
(121) Marchi, M. *J. Phys. Chem. B* **2003**, *107*, 6598.
(122) Tarek, M.; Tobias, D. J. *Biophys. J.* **2000**, *79*, 3244.
(123) Xia, T.; Becker, H. C.; Wan, C.; Frankel, A.; Roberts, R. W.; Zewail, A. H. *Proc. Natl. Acad. Sci. U.S.A.* **2003**, *100*, 8119.

(124) Kamal, J. K. A.; Xia, T.; Pal, S. K.; Zhao, L.; Zewail, A. H. *Chem. Phys. Lett.* **2004**, *387*, 209.
(125) Schmitke, J. L.; Stern, L. J.; Klibanov, A. M. *Proc. Natl. Acad. Sci. U.S.A.* **1997**, *94*, 4250.
(126) Zou, S. Z.; Baskin, J. S.; Zewail, A. H. *Proc. Natl. Acad. Sci. U.S.A.* **2002**, *99*, 9625.
(127) Wan, C.; Fiebig, T.; Kelley, S. O.; Treadway, C. R.; Barton, J. K.; Zewail, A. H. *Proc. Natl. Acad. Sci. U.S.A.* **1999**, *96*, 6014.
(128) Fiebig, T.; Wan, C.; Kelley, S. O.; Barton, J. K.; Zewail, A. H. *Proc. Natl. Acad. Sci. U.S.A.* **1999**, *96*, 1187.
(129) Fiebig, T.; Wan, C.; Zewail, A. H. *ChemPhysChem* **2002**, *3*, 781.
(130) Qu, X. G.; Wan, C.; Becker, H. C.; Zhong, D. P.; Zewail, A. H. *Proc. Natl. Acad. Sci. U.S.A.* **2001**, *98*, 14212.
(131) Zhong, D. P.; Douhal, A.; Zewail, A. H. *Proc. Natl. Acad. Sci. U.S.A.* **2000**, *97*, 14056.
(132) Steiger, B.; Baskin, J. S.; Anson, F. C.; Zewail, A. H. *Angew. Chem., Int. Ed.* **2000**, *39*, 257.
(133) Zhong, D. P.; Zewail, A. H. *Proc. Natl. Acad. Sci. U.S.A.* **2001**, *98*, 11867.
(134) Zhong, D.; Pal, S. K.; Wan, C.; Zewail, A. H. *Proc. Natl. Acad. Sci. U.S.A.* **2002**, *99*, 11873.
(135) Douhal, A.; Kim, S. K.; Zewail, A. H. *Nature (London)* **1995**, *378*, 260.
(136) Chachisvilis, M.; Fiebig, T.; Douhal, A.; Zewail, A. H. *J. Phys. Chem. A* **1998**, *102*, 669.
(137) Fiebig, T.; Chachisvilis, M.; Manger, M.; Zewail, A. H.; Douhal, A.; Garcia-Ochoa, I.; Ayuso, A. D. H. *J. Phys. Chem. A* **1999**, *103*, 7419.
(138) Baskin, J. S.; Yu, H. Z.; Zewail, A. H. *J. Phys. Chem. A* **2002**, *106*, 9837.
(139) Yu, H. Z.; Baskin, J. S.; Zewail, A. H. *J. Phys. Chem. A* **2002**, *106*, 9845.
(140) Pal, S. K.; Zhao, L.; Xia, T.; Zewail, A. H. *Proc. Natl. Acad. Sci. U.S.A.* **2003**, *100*, 13746.
(141) Zhao, L.; Pal, S. K.; Xia, T.; Zewail, A. H. *Angew. Chem., Int. Ed.* **2004**, *43*, 60.
(142) O'Neill, M. A.; Becker, H.-C.; Wan, C.; Barton, J. K.; Zewail, A. H. *Angew. Chem., Int. Ed.* **2003**, *42*, 5896.
(143) Teng, M.; Usman, N.; Frederick, C. A.; Wang, A. H. J. *Nucleic Acids Res.* **1988**, *16*, 2671.

CR020689L